UPGRADING THE MONARCH OPERATIONAL FORECAST:
DEPLOYMENT PROTOCOL AND DUST EMISSION UPGRADES OVER NAMEE

BDRC-2020-001

Sara Basart, Carlos Pérez García-Pando[*],
Oriol Jorba, Francesco Benincasa, Miriam
Olid, Kim Serradell, Gilbert Montanyé

Barcelona Supercomputing Center, BSC
(*)Catalan Institution for Research and Advanced Studies, ICREA

Ernest Werner

Spanish State Meteorological Agency, AEMET

30 November 2020

TECHNICAL REPORT

Series: Barcelona Dust Regional Center (BDRC) Technical Report

A full list of BDRC Publications can be found on our website under:

http://dust.aemet.es/

Summary

The present document describes the technical protocol for upgrading the MONARCH model configuration used in the WMO Barcelona Dust Forecasting Center. The operational workflow of the WMO Barcelona Dust Forecast Center considers the execution of the model in two HPC clusters, one in BSC (MareNostrum 4) and a backup in AEMET (Nimbus). Also, the document presents a detailed model description of the upgraded MONARCH model configuration and its performance. This upgraded MONARCH version is the operational version since **December 2020** in the WMO Barcelona Dust Forecast Center.

Contents

1. Deployment protocol

Once the new features have been implemented and tested in the MONARCH model (see Section 2), the model version resulting will be thoroughly evaluated and compared with the performance of the daily dust forecast in the WMO Barcelona Dust Forecast Center.

The complete deployment protocol includes the following phases:

- Benchmark
- Installation
- Pre-operational
- Operational

Each of the mentioned phases is described in detail in the next Sections.

1.1. Benchmark

Before a system upgrade of the WMO Barcelona Dust Forecast Center forecasting system is implemented, extensive testing of the new system is carried out. The results of the upgraded version of the model of the **latest complete two years** will be evaluated and compared with the current model version. This benchmark testing will help us to identify the weaknesses of the model and also provides an assessment of the model performance and uncertainties.

The model outputs will be evaluated for dust optical depth (at 550nm, DOD) and surface PM10 observations. The standard metrics that are used to quantify the mean departure between modelled (c_i) and observed (o_i) quantities are the Mean Bias Error (MB), the Root Means Square Error (RMSE), the correlation coefficient (r) and the Fractional Gross Error (FGE). They are presented in Table 1.1, where n denotes the number of data.

Table 1.1. *Summary of the statistical metrics that will be used in the model evaluation.*

Statistic Parameter	Formula	Range	Perfect score	Description
Mean Bias Error (MB)	$MB = \frac{1}{n}\sum_{i=1}^{n}(c_i - o_i)$	∞ to $+\infty$	0	It captures the average deviations between the two datasets. It has the units of the variable. Values near 0 are the best; negative values indicate underestimation and positive values indicate overestimation.
Root Mean Square Error (RMSE)	$RMSE = \sqrt{\frac{1}{n}\sum_{i=1}^{n}(c_i - o_i)^2}$	0 to $+\infty$	0	It combines the spread of individual errors. It is strongly dominated by the largest values, due to the squaring operation. Especially in cases where prominent outliers occur, the usefulness of RMSE is questionable, and the interpretation becomes more difficult.
Correlation coefficient (r)	$r = \frac{\sum_{i=1}^{n}(c_i - \bar{c})\cdot(o_i - \bar{o})}{\sqrt{\sum_{i=1}^{n}(c_i - \bar{c})^2}\cdot\sqrt{\sum_{i=1}^{N}(o_i - \bar{o})^2}}$	-1 to 1	1	It indicates the extent to which patterns in the model match those in the observations.
Fractional Gross Error (FGE)	$FGE = \frac{2}{n}\sum_{i=1}^{n}\left|\frac{c_i - o_i}{c_i + o_i}\right|$	0 to 2	0	It is a measure of model error, ranging between 0 and 2 and behaves symmetrically with respect to under- and overestimation, without overemphasising outliers.

The overall skills scores of the candidate model version will be analysed in detail in terms of column-load (i.e. DOD) and surface concentration (PM10) by the scientific-expert group in charge

of the operational model. The main criteria will be: 1) the performance is consistent across regions, seasons and parameters, and 2) it should show equal or better overall performance than the operational version at least in one of the skills scores (i.e. correlation coefficient, MB, RMSE and FGE) without noticeably degrading the other over the NAMEE region. The **scientific-expert group will take the final decision** of approving and transferring to operations this candidate model configuration.

1.2. Installation

Installation phase considers the compilation of the source code of the model and the associated workflow manager that will launch the daily execution in the operational machines of the WMO Barcelona Dust Forecast Center (i.e. MareNostrum 4 and Nimbus) and the version control system.

The different versions of the BSC in-house model MONARCH and the scripts to execute it (i.e. the associated **workflow manager**) are centralised in **GitLab,** which is the version control system used at BSC. The operational model version will be identified by a Tag so the operational configuration can be reproduced when necessary from scratch.

Autosubmit is a python-based tool developed and maintained at the BSC to create, manage and monitor experiments by using Computing Clusters, HPC's and Supercomputers remotely via ssh. It has support for experiments running in more than one HPC and for different workflow configurations (see references in https://autosubmit.readthedocs.io/en/latest/).

The experiment is defined as a sequence of jobs, including compiling, sending data or running the simulation. *Autosubmit* remotely submits and manages this sequence of jobs in a transparent way for the user. The experiment will be identified using an experiment identifying (**experiment ID**) assigned by *Autosubmit* when the experiment is created. The experiment ID is related to a specific version and configuration of the model.
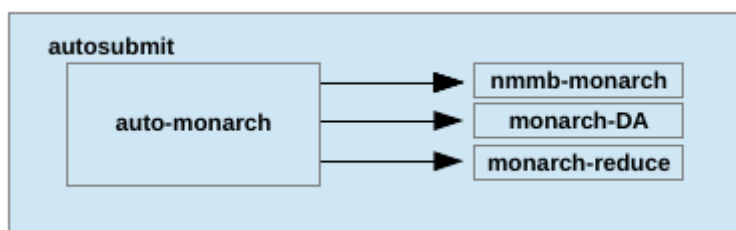
Figure 1.1. *Schematic diagram of module and sub-modules of the Auto-MONARCH run in the Autosubmit workflow manager environment. This includes the experiment workflow manager Auto-MONARCH, the chemical-weather system MONARCH (i.e. nmmb-monarch), the MONARCH assimilation scheme (i.e. monarch-DA), and the post-processing tool (i.e. monarch-reduce that includes interpolations and the calculations of some diagnostics)*

Autosubmit will also be used to run the WMO Barcelona Dust Forecast Center through a set of

scripts and templates developed under **Auto-MONARCH** project (available in the BSC git repository, (https://earth.bsc.es/gitlab/es/auto-monarch.git). Auto-MONARCH allows us to optimise the protocol for installing a new model version and post-processing in future upgrades. The set of post-processing tools (for variable extraction, statistics calculations and interpolation/regridding) has been highly improved, from the-point-of-view of performances (i.e. parallelisation) and "big-data" handling, to face in an optimal way the increasing resolution.
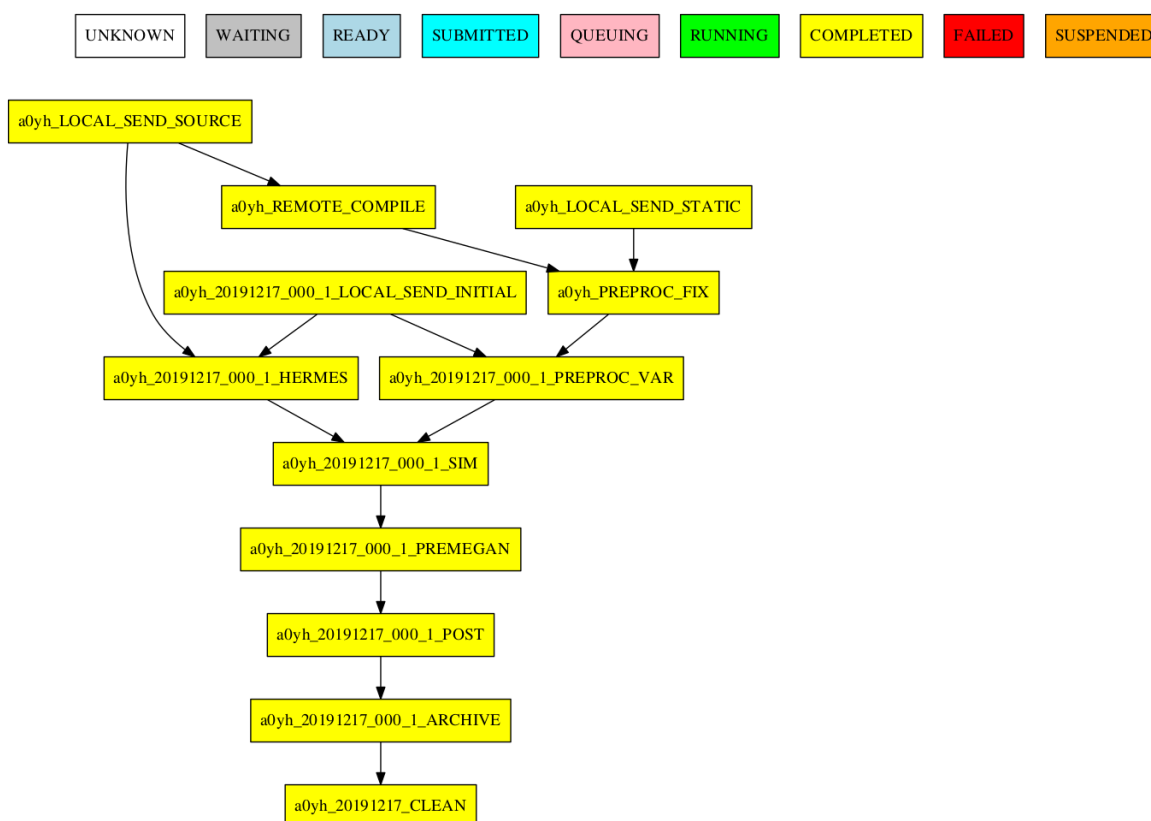
Figure 1.2. *Example of an experiment run by Auto-MONARCH.*

The whole deployment of the model in the two considered HPC machines (MareNostrum 4 and Nimbus) would be performed by *Autosubmit* and Auto-MONARCH.

- **MareNostrum4:** The whole deployment, extensively tested in MareNostrum 4, is performed by Auto-MONARCH workflow. The scheduling of model runs will be managed by a cron job from a virtual machine which will launch *Autosubmit* using the Auto-MONARCH workflow and run the simulation.

- **Nimbus:** The same approach as in MareNostrum 4 is applied in Nimbus. In this case, minor

adaptations (mainly in tasks "REMOTE_COMPILE" and "LOCAL_SEND_INITIAL") have to be done to the current workflow to be able to run in Nimbus. It is used as an independent *Autosubmit* instance (installed in AEMET virtual machine), and Auto-MONARCH will be applied to the Nimbus cluster.

Once deployments in the different platforms have been fully tested, future updates of model source code can be performed easily defining new experiment IDs in the workflow manager.

As the last step, a comparison of the results of the model in both machines (i.e. MareNostrum 4 and Nimbus) will be made. A daily run of 72-hours forecasts with the same meteorological initial and boundary conditions and starting with a 'cold start' (i.e. initial dust concentration field at 0) from the two clusters will be compared to check their consistency. In this comparison, we will include all the meteorological and dust parameters.

1.3. Pre-operational

To check and validate the consistency of the daily execution as well as the results of the model's upgrade there will be a parallel execution in MareNostrum 4 and Nimbus. These runs will use a different experiment ID from the operational run.

The operational run will be executed every day as the operational forecast in MareNostrum 4 (using the reservation nodes) and Nimbus. The parallel runs will be conducted when the operational run finishes to try not to affect the daily execution. These parallel executions will be run for three months (at least) in both machines (i.e. MareNostrum 4 and Nimbus).

During this period, there will be an internal webpage that will show the daily comparison of the two runs in MareNostrum and Nimbus for an everyday quick look. In addition, at the end of this 3-months period, the skills scores and the execution performance of both model versions will be compared. For the assessment, it will be considered:

- Number of days that the daily execution failed (< 2%)
- Skill scores of the comparison with AERONET observations

Once the scientific responsible will confirm that the upgraded model version is stable in the different platforms, and its performance is comparable to the benchmark phase, the operational run can be replaced with this parallel run. This is considered in the **operational phase** (see Section 1.4).

1.4. Operations

After the pre-operational phase (Section 1.3), i.e. once it is checked that the upgraded model version is stable in the different platforms and its performance is comparable to the benchmark

phase; the upgraded model configuration will be considered as operational version, and it will be used for the daily dust service in the WMO Barcelona Dust Forecast Center.

The date in which the updated version will move to operations **will be agreed by the BSC scientific-technical group**. The decided day, the operational run will be replaced with this parallel run, and a new Tag will be created in the GitLab *Auto-MONARCH* project for keeping track of the change.

2. MONARCH's upgrade

2.1. Model's overview

The Multiscale Online Nonhydrostatic AtmospheRe CHemistry model (**MONARCH**), developed at the Barcelona Supercomputing Center (BSC), is an online meteorology-chemistry model that provides short- and mid-term chemical weather forecasts on both regional and global scales (Pérez et al., 2011; Haustein et al. 2012; Jorba et al. 2012; Spada et al. 2013; Spada et al. 2015; Badia and Jorba 2015; Badia et al. 2016; Badia et al. 2017; Di Tomaso et al. 2017). The MONARCH is based on the online coupling of the meteorological Nonhydrostatic Multiscale Model on the B-grid (NMMB; Janjic and Gall, 2012) developed at the National Centers for Environmental Prediction (NCEP), with a full chemistry module, including gas phase and all aerosol species, developed at the BSC. Therefore, the model is designed to account for the feedback among gases, aerosol particles and meteorology. The aerosol module is enhanced with data assimilation (DA) system to optimally combine forecasts with observations and improve predictions. A schematic description of the MONARCH modelling system is presented in Figure 2.1.1.
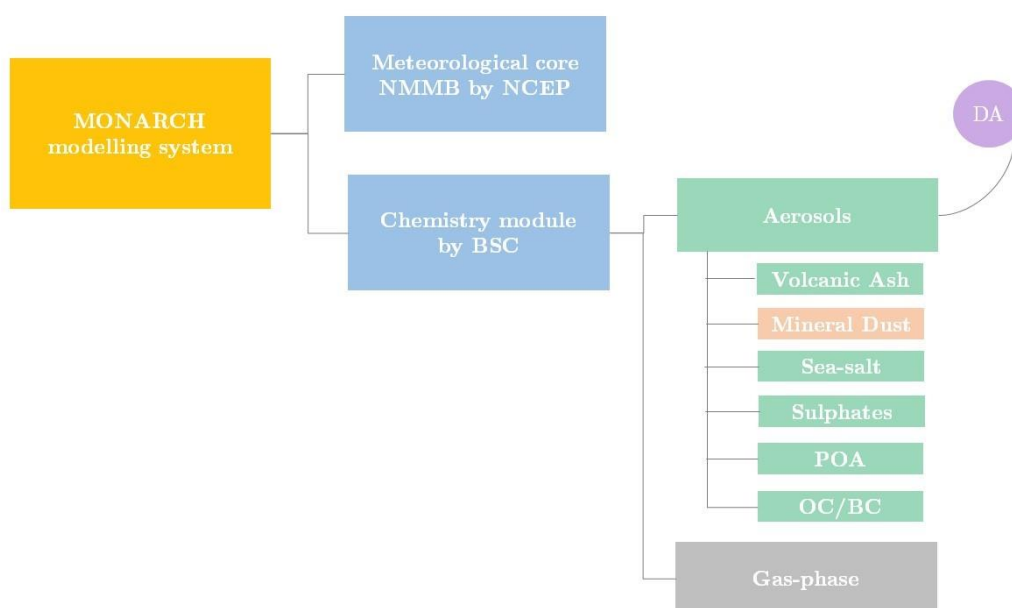
Figure 2.1. *Scheme of the main modules of the Multiscale Online Nonhydrostatic AtmospheRe*

CHemistry model (MONARCH) model.

The desert dust module, previously known as NMMB/BSC-Dust that is embedded into the NMMB meteorological core, solves the mass balance equation for dust taking into account the following processes: i) dust generation and uplift by the wind, ii) horizontal and vertical advection, iii) horizontal diffusion and vertical transport by turbulence and convection, iv) dry deposition and gravitational settling, v) wet removal, including in-cloud and below-cloud scavenging. The model includes eight dust size bins; sub-micron particles in bins 1-4 correspond to clay originated particles, while the remaining particles in bins 5-8 to silt (Pérez *et al.*, 2006).

The desert dust component of the MONARCH model has been evaluated at regional and global scales (Pérez *et al.*, 2011; Haustein *et al.*, 2012). Pérez et al. (2011) provide daily to annual evaluations of the model for its global and regional configurations. At the global scale, the model lies within the top range of AEROCOM dust models in terms of performance statistics for surface concentration, deposition and aerosol optical depth (AOD). At the regional scale, the model reproduces significantly well the daily variability and seasonal spatial distribution of the dust optical depth (DOD) over Northern Africa, the Middle East and Europe. In Haustein et al. (2012), the model was evaluated at the regional scale against measurements at source regions from the Saharan Mineral Dust Experiment (SAMUM-I) and the Bodélé Dust Experiment (BoDEx) campaigns. Gama et al. (2015) and Ansman et al. (2017) show the availability of the model to reproduce seasonal transport over the North Atlantic.

The MONARCH model is the reference model of the WMO Barcelona Dust Forecast Center, while the model also contributes to the WMO SDS-WAS regional dust multi-model ensemble and the ICAP global operational aerosol multi-model ensemble.

2.2. New features: Dust emissions

The identification of dust sources is one of the crucial aspects of representing dust mobilisation in models. Traditionally, models used aridity as a criterion to identify potential dust sources. Satellite retrievals subsequently showed that the most prolific sources occupy only a small fraction of arid regions. These so-called 'preferential sources' are found within enclosed basins, were easily eroded soil particles have accumulated after fluvial erosion of the surrounding highlands. The implementation of preferential source functions based on topography (Ginoux et al. 2001) has significantly improved the skill of models by approximately locating large-scale natural sources. However, this approach is limited for representing small-scale dust sources and regions where the main sources are anthropogenic (cropland and pasture), which can make a significant contribution to the dust load.

We have implemented a new high-resolution mapping of dust sources based on high-resolution MODIS Collection (Ginoux et al., 2012) within the model. The new source map provides the frequency of occurrence (FoO) of dust optical depth > 0.2 based on MODIS Deep Blue Collection 6 and distinguishes between natural and anthropogenic (primarily agricultural) dust sources based on high-resolution land-use datasets. The model contains now multiple choices to treat

dust sources and emission. In addition to the standard emission scheme, new options are now available. In order to constrain the threshold for dust emission, we implemented drag partition schemes based on satellite data.

2.2.1. Model developments

In addition to the standard emission scheme in MONARCH based on a variation of Marticorena and Bergametti (1995), **six additional emission schemes** are now available in the model: the GOCART scheme from Ginoux et al. (2001), four schemes that represent dust emission through saltation bombardment and aggregate disintegration (Shao, 2001; Shao, 2004; Shao et al., 2011, Kok et al., 2014) and one scheme represents aerodynamic dust entrainment (Klose et al., 2014).

A key aspect for calculating dust emission is the **threshold of a surface wind speed or friction velocity that must be exceeded for dust emission**. Models have generally neglected the effect of roughness on wind erosion because this inhibition depends upon local environmental parameters that are not well known. For example, environmental contrasts between natural and cultivated regions are large, and therefore we need a physically-based model of the threshold that accounts for these differences. Our approach has been to assume that the roughness is controlled predominantly by variables that are related to satellite retrievals with high spatial resolution. The effect of **roughness elements** is to reduce the force of the wind on the erodible soil particles. In models, this shielding can be represented by a reduction in the surface wind stress. Alternatively, Marticorena and Bergametti (1995) proposed that the threshold for emission be increased. In this scheme, the threshold wind stress for wind erosion u_T^* is represented by u_{TS}^*, the threshold of a smooth surface with a correction f_{eff} accounting for surface roughness:

$$u_T^* = \frac{u_{TS}^*}{f_{eff}}$$

The correction f_{eff} decreases as the surface gets rougher, so that stronger wind stress is needed to mobilise soil particles. We have derived a global version of f_{eff} for non-erodible roughness elements and vegetation cover based on:

1) In arid regions, we used a static roughness (at 0.1º) taken from Prigent et al. (2012), who combined satellite microwave backscatter (ASCAT) with visible/near-infrared reflectances (PARASOL).
2) In semi-arid regions with natural vegetation and cultivated areas, we estimated a dynamic roughness based on the dimensions of vegetation characterised using the MODIS Leaf Area Index (LAI, at 0.10º).

The use of MODIS LAI allows the emission threshold to vary throughout the growing season. The correction u_T^* is largest (and f_{eff} is smallest) for roughness elements like stones or vegetation that are tall and closely spaced. While incorporating these dependencies, there is uncertainty related to characterising the height or spacing of roughness elements, mainly where they are of irregular

size or spacing.

In addition, we also implemented a **frontal-area-index based parameterisation** for all dust emission schemes based on fractional vegetation cover from photosynthetic and non-photosynthetic vegetation (at 0.05º) derived from MODIS based on Guerschman et al. (2015).

Furthermore, new developments refer to the refinement of the description of the **desert dust source map**. The baseline preferential source map used in the model describes the sources as a function of topography (see Figure 2.2.1; Ginoux et al., 2001). With this approach, enclosed basins are considered preferential dust sources based on the assumption that easily eroded soil particles have accumulated after fluvial erosion of the surrounding highlands. We implemented and tested a new dust source map that **combines the Moderate Resolution Imaging Spectroradiometer (MODIS) Deep Blue (DB) with a land-use database**. This map is derived from measurements of AOD, Angstrom exponent, and single scattering albedo following Ginoux et al. (2012) and has been adapted to MODIS Collection 6. The map provides the frequency of occurrence of Dust Optical Depth (DOD) greater than 0.2 (Figure 2.2.1).
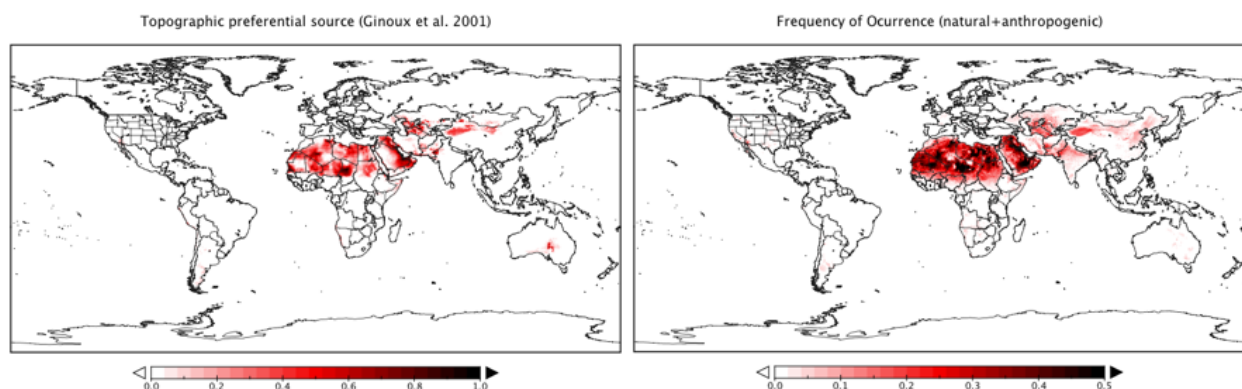
Figure 2.2.1. *Topographic preferential source (Ginoux et al. 2001) (left). Frequency of Occurrence (FoO) of DOD > 0.2 based on MODIS Deep Blue Collection 6 (Ginoux et al., 2012) (right).*

2.2.2. Sensitivity tests

For testing the different options available in the model, we have run sensitivity simulations for the year 2016 with **two different dust emission schemes** as well as different **desert dust source functions**.

- **Dust emission schemes** considered are Ginoux et al. (2001, referred to **G01**) and the scheme of Kok et al. (2014, referred to **K14**). G01 is semi-empirical, heavily relies on the topographic preferential source mask and is not very sensitive to soil humidity. K14 is theoretically based, heavily depends on the input clay fraction dataset and is very sensitive to soil humidity.
- **Desert dust source functions** considered are the classic topographic preferential source

from Ginoux et al., (2001, referred as **TOPO source**) and the second one using the MODIS frequency of occurrence of DOD > 0.2 as preferential source (Ginoux et al., 2012, referred as **MODIS source**).

For the set of sensitivity analysis, we have run sensitivity simulations **for the year 2016** and will focus on improving the annual dust cycle in the **Middle East and the Eastern Mediterranean** that it is the regions where the current operational MONARCH version presents some limitations as it is shown in the evaluation of the WMO Barcelona Dust Forecast Center (https://dust.aemet.es/forecast-evaluation).

In the sensitivity runs, we have included three nested domains (see Figure 2.2.2): a large domain (D01) at 0.27˚ (~27 km) resolution, a domain covering the Arabian Peninsula and Turkey at 0.09˚ (~9 km) resolution, and a small domain covering Kuwait and neighbouring regions to the west at 0.03˚ (~3km) resolution. The design also searches to see the impact of the spatial resolution in the model results. In this report, we show the evaluation with AERONET of a couple of sensitivity experiments with different emission schemes for D01 and D02.
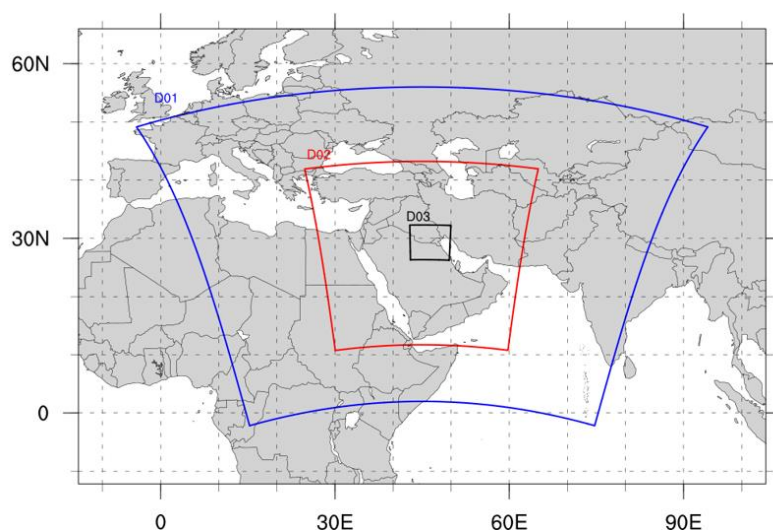
Figure 2.2.2. *Three nested domains for K-Dust forecasts. D01 at 0.27˚, D02 at 0.09˚, and D03 at 0.03˚.*

The simulated dust distributions consist of daily runs, and the initial state of the dust concentration is defined by the 24-h forecast of the previous-day model run. Only in the 'cold start' of the model, concentration is set to zero. The cold start of the model is initiated on 1st January 2015 to also include the spin-up of the soil moisture (that requires a year). The ERA-Interim, which is a global weather reanalysis produced by the European Centre for Medium-Range Weather Forecasts (ECMWF) at 0UTC are used as initial meteorological conditions and boundary conditions at intervals of 6 h. The resolution of the model is set to 40 layers extending up to approximately 15 km in the vertical.

2.2.2.1. Evaluation strategy

In order to evaluate the performance of the model forecasts, we will use dust-filtered AERONET observations. High quality aerosol optical properties are provided by the ground-based sun-/sky photometer networks of AERONET (Aerosol, Robotic NETwork; Holben, 2001: http://aeronet.gsfc.nasa.gov/) programme. The AERONET program provides a long-term, continuous and readily accessible public domain database of aerosol optical, microphysical and radiative properties for aerosol research and characterisation, validation of satellite retrievals, validation of aerosol models, and synergism with other databases. The network imposes standardisation of instruments, calibration, processing and distribution.

Solar extinction measurements are used to compute **aerosol optical depth (AOD)** at each wavelength, except for the 940 nm channel, used to retrieve precipitable water vapour (Eck et al., 1999). Ångström Exponent (AE), which is a measure of the AOD spectral dependence with the wavelength of the incident light, is a qualitative indicator of the aerosol's predominant particle size and it can be computed for two or more wavelengths (Schuster et al., 2006). The AOD uncertainty is approximately 0.01–0.02 (spectrally dependent, with higher errors in the UV) and it alters the AE by 0.03–0.04 (Eck et al., 1999; Schuster et al., 2006). Data acquisition protocols, calibration procedures and data processing methods have been extensively described (Holben et al., 1998; Dubovik et al., 2000; Smirnov et al., 2000; O'Neill et al., 2003). The instrument is out of operation for some weeks while necessary yearly calibration is carried out. Consequently, the data coverage in a given station is typically limited to 100–250 days per year. This data is provided in three categories: 1) raw (level 1.0), 2) cloud-screened (level 1.5) following the methodology described by Smirnov et al. (2000), and 3) cloud-screened and quality-assured (level 2.0).

The dust-filtering considered here is based on the Spectral Deconvolution Algorithm (SDA, also known as O'Neill) AERONET products that provide AODcoarse and AODfine products. AODcoarse observations are fundamentally associated with maritime/oceanic aerosols and desert dust. Since sea-salt is related to low AOD (< 0.03; Dubovik et al., 2002) and mainly affects coastal stations, high AODcoarse values are mostly related to mineral dust (i.e. DODcoarse).

Discrete statistics such as correlation coefficient (r), fractional gross error (FGE), root mean square error (RMSE) and mean bias (MB) measure the skill of the model when performing diagnostic analyses of dust AOD at specific points where AERONET sites are located. The description of these statistics can be found in Table 1.1. Because AERONET data are acquired at 15-min intervals on average, all AERONET measurements within ±90 min of the model outputs have been extracted and used for the model comparison on a 3-hourly basis. Finally, for the present evaluation exercise, **we use the SDA Version 3 cloud-screened (Level 1.5) observations**. These observations are used for operational evaluation purposes in the WMO Barcelona Dust Forecast Center. The AERONET sites considered for evaluating the proposed sensitivity tests are shown in Figure 2.2.3.
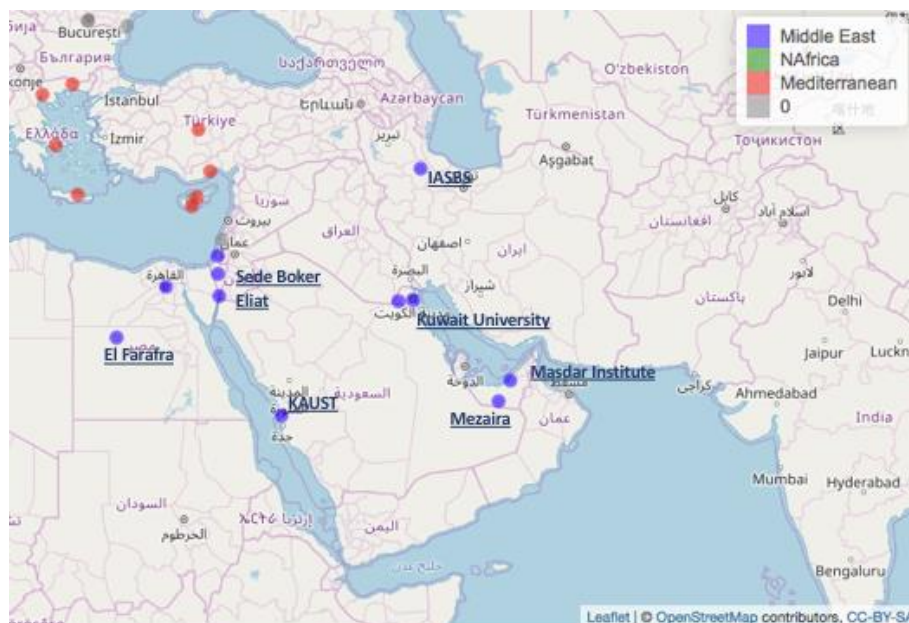
Figure 2.2.3. *Geographical distribution of the considered AERONET sites. The selected sites correspond to those in the Middle East (marked in blue)*

2.2.2.2. Model's results

Our simulations show that the first (at ~ 27 km horizontal spatial resolution) and second (at ~ 9 km horizontal spatial resolution) domain gave similar and satisfactory results (see the resulting skill scores per AERONET site in Figure 2.2.4). Differences in the results of both domains are mostly related to the inclusion of Saharan dust sources in the domain of simulation. This is evident in the comparison of the El Farafra (Egypt) and CUT-TEPAK (Turkey) AERONET sites where the second domain (D02, in blue in Figure 2.2.4) is strongly overestimating the observations along the year. Therefore, since here, we will consider **the results of the extended domain** (D01 in red in Figure 2.2.4) for the analysis.

In the AERONET comparison in the Middle East (see Figure 2.2.4), G01 is providing significantly better results overall in comparison with K14. The G01 can reproduce the annual cycle, and the associated annual correlation is generally very good (r > 0.65). However, for Kuwait University and Mezaira AERONET sites, the results show overestimation in the summer and particularly in Kuwait, there is a decrease in the correlation (r ~0.4).
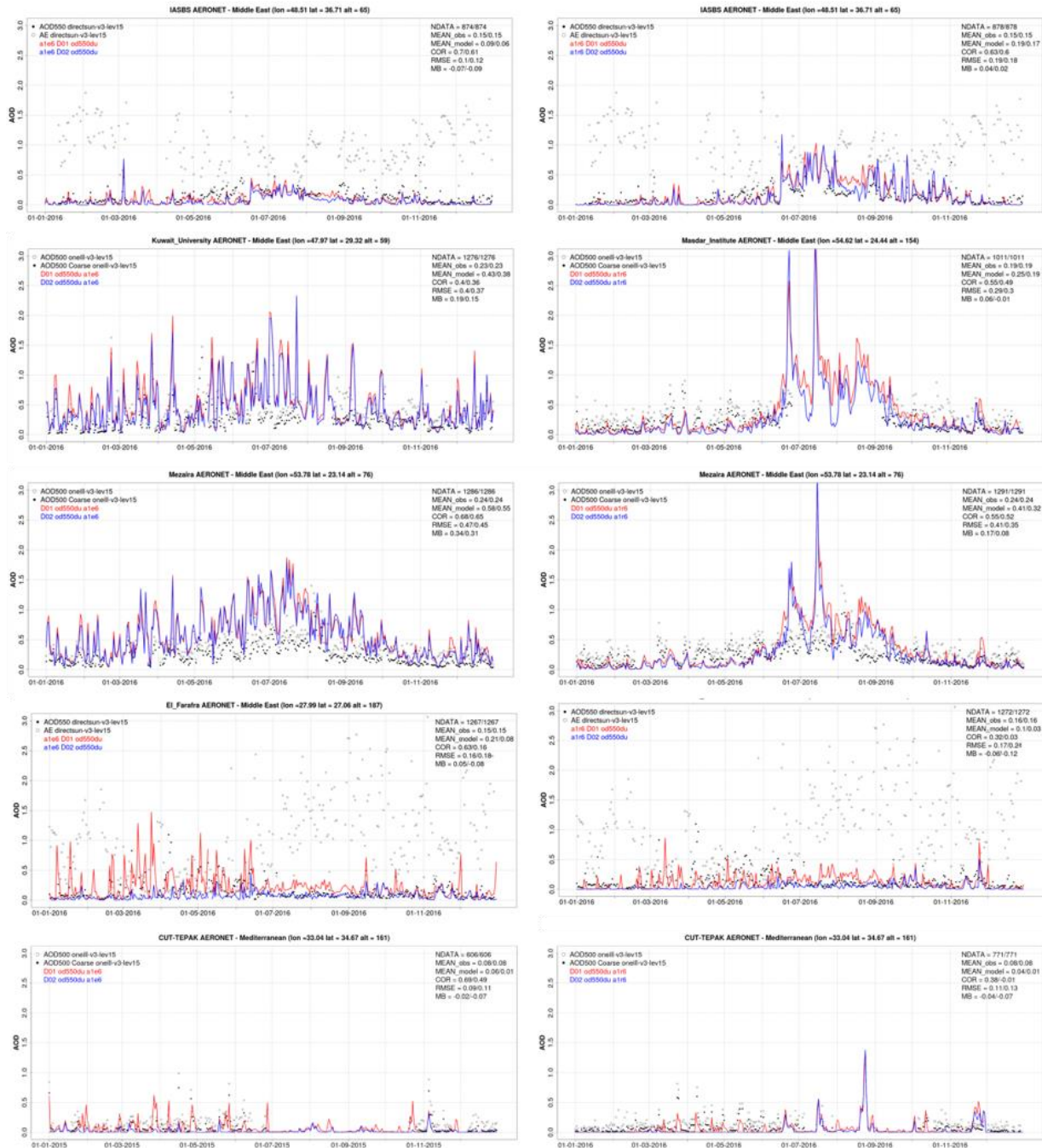
Figure 2.2.4. *Time series for modelled dust optical depth (DODcoarse) and dust-filtered AOD observations from AERONET (i.e. AODcoarse = DODcoarse) including skill scores. The selected AERONET sites are Eilat (Israel), KAUST Campus (Saudi Arabia), Mezaira (United Arab Emirates), El Farafra (Egypt) and CUT-TEPAK (Turkey). Their location is shown in Figure 2.5. For the same AERONET site, the evaluation of G01 is on the left and the evaluation of K14 on the right. In each time series, it is shown the results of the D01 (in red) and D02 (in blue).*

In the last round of simulations, we compare the newly implemented MODIS based preferential source (MODIS source, see Section 2.1.1) with the default source map based on the topographical approach (TOPO source, see Section 2.1.1) implemented in the current operational version of the WMO Barcelona Dust Forecast Center. For these experiments, it is used G01 and the extended D01 domain for both experiments, i.e. TOPO source and MODIS source. The results of the AERONET comparison are shown in Figure 2.2.5 and Figure 2.2.6.
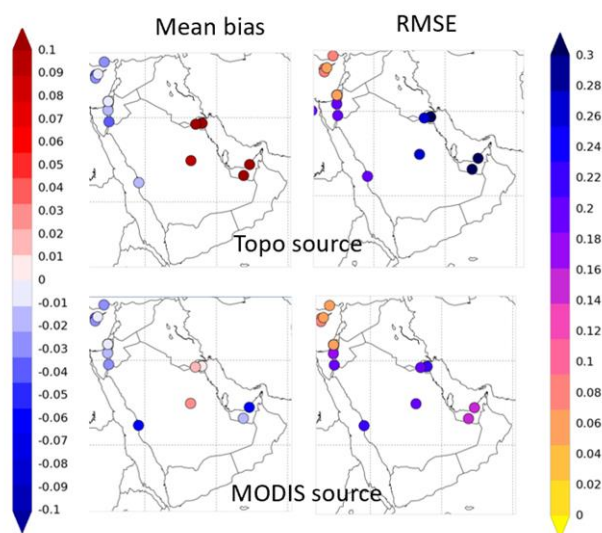
Figure 2.2.5. *Evaluation results with AERONET SDA products for 2016. On the left: Map showing the overall Mean Bias (MB). On the right: Root Mean Square Error (RMSE) for the two simulations, using the TOPO source (first row) or the MODIS source (second row).*

For all stations in the Middle East, it is observed that the MODIS source improved the statistical skills (see MB < 0.01 and RMSE < 0.20 in Figure 2.2.5) in all cases. Also, for the AERONET stations of Kuwait University, Masdar Institute and Mezaira, MODIS source had less overestimation in AOD in summer than the high overestimations with TOPO source and better correlation coefficients (see Figure 2.2.6).
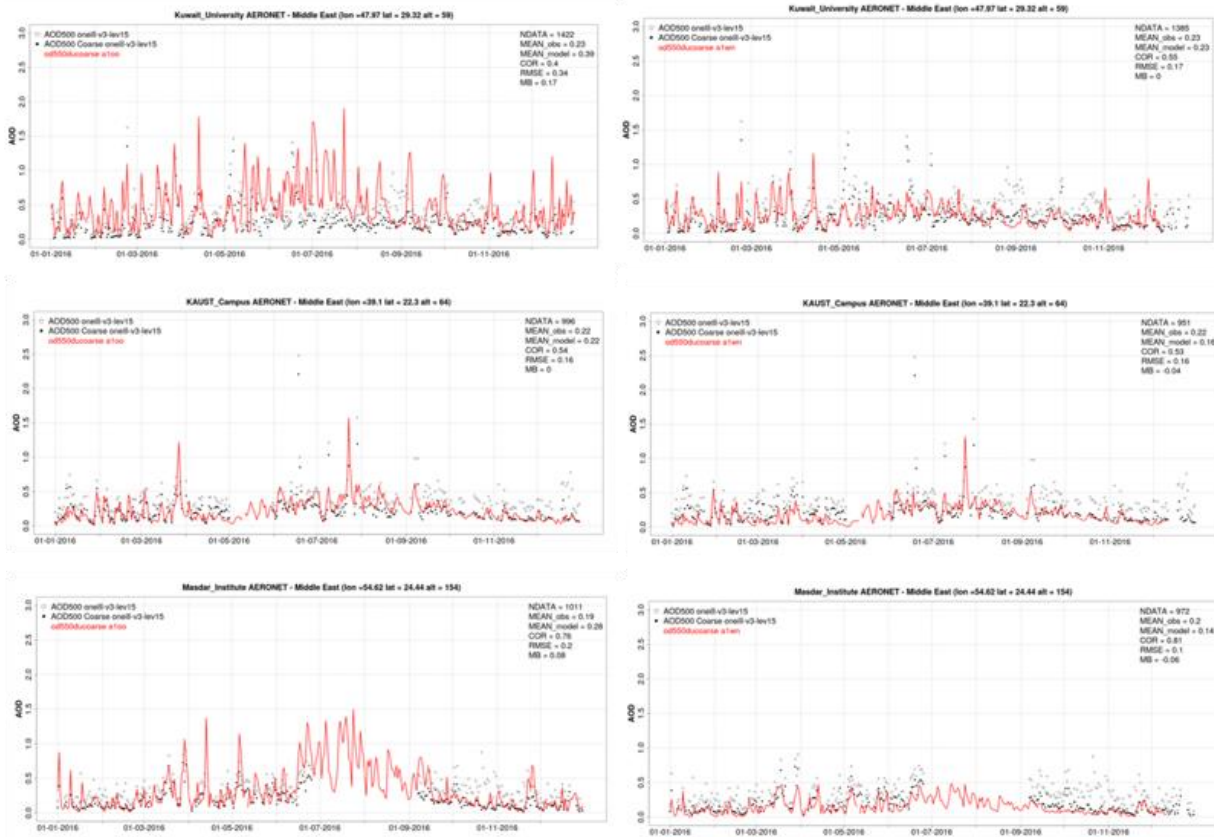
Figure 2.2.6. *Time series for modelled dust optical depth (DODcoarse) and dust-filtered AOD observations from AERONET (i.e. AODcoarse = DODcoarse) including skill scores. The selected AERONET sites are Kuwait University (first row), KAUST Campus (second row) and Masdar Institute (third row). For the same AERONET site, the evaluation of TOPO source is on the left and the evaluation of MODIS source on the right.*

2.2.3. Annual DOD evaluation over NAMEE

Considering the results of these sensitivity experiments, the proposed experimental model configuration that we will evaluate here includes **G01 and MODIS source** at 0.10^0 x 0.10^0 covering North Africa, Middle East and Europe, NAMEE (fully described in Section 2.1). In this section, we will present the annual results for NAMEE of the proposed experimental run and its comparison with dust-filtered DOD and DODcoarse AERONET observations (Version 3 Level 1.5) for the year 2016. The details of the dust-filtering applied to the AERONET observations is described in Section 2.2.2.1.

The simulated dust distributions consist of daily runs, and the initial state of the dust concentration is defined by the 24-h forecast of the previous-day model run. Only in the 'cold start' of the model, concentration is set to zero. The cold start of the model is initiated on 1st January 2015 to also include the spin-up of the soil moisture (that requires a year). The ERA-Interim, which is a global

weather reanalysis produced by the European Centre for Medium-Range Weather Forecasts (ECMWF) at 0UTC are used as initial meteorological conditions and boundary conditions at intervals of 6 h. The resolution of the model is set to 40 layers extending up to approximately 15 km in the vertical.

In comparison with AERONET (see Figure 2.2.7), this experimental run can reproduce the DOD and DODcoarse daily variability with an annual overall correlation coefficient of 0.76 and 0.74, respectively for DOD and DODcoarse, with higher values in long-transport regions as the Mediterranean (with 0.75 and 0.79, respectively for DOD and DODcoarse). Overestimations are observed in desert dust regions. MB in North Africa and the Middle East is 0.03 for DOD and DODcoarse. Otherwise, underestimations are observed in the Mediterranean and in the Guinea Gulf. Particularly in the Mediterranean, DODcoarse is larger underestimated in comparison with the DOD.
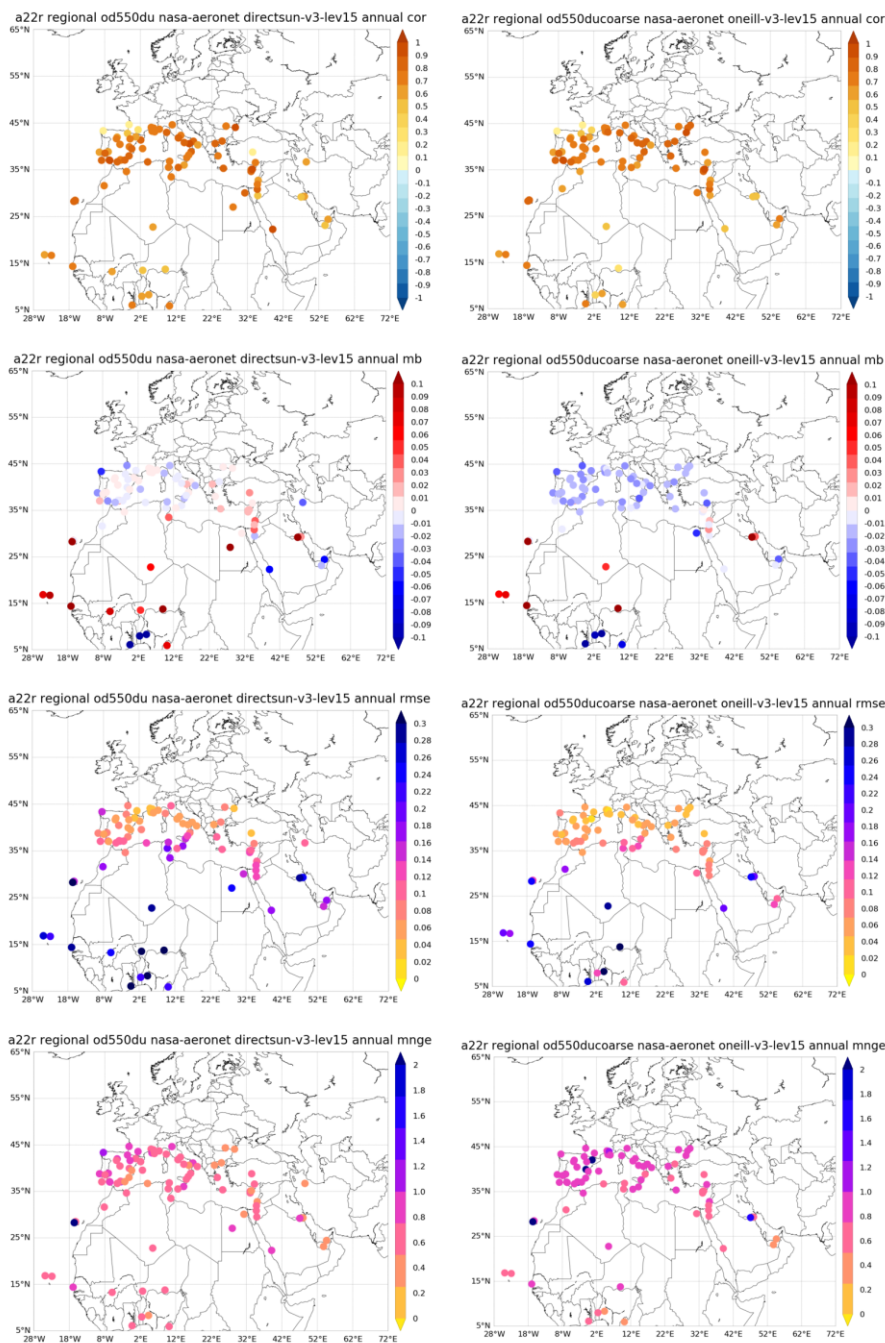
Figure 2.2.7. *Skill scores (correlation coefficient and MB) for 24-hour forecasts (at 3-hourly basis) of MONARCH experimental run. DOD (left column) and DODcoarse for **2016**. For DOD, dust-filtered AERONET dust observations (i.e. dust observations when AE < 0.75 and no-dust observations when AE > 1.2) is the reference meanwhile for DODcoarse, AODcoarse from SDA AERONET is considered.*

2.2.4. *Model configuration proposed*

In addition, an extra **sensitivity analysis of the meteorological global initial and boundary conditions** was done for five months in 2019 (from August to December). In this test, it was considered the same model configuration (using **G01 and MODIS source** at 0.10⁰ x 0.10⁰ covering North Africa, Middle East and Europe, NAMEE, domain) but different horizontal resolutions (0.25⁰ vs 0.50⁰) of the Global Forecast System (GFS) which is a weather forecast model produced by the National Centers for Environmental Prediction (NCEP). GFS at 12 UTC is used as initial meteorological conditions and boundary conditions at intervals of 6 h. The overall comparison over NAMEE with AERONET shows similar results ($r = 0.73$, MB = 0.03, RMSE = 0.14 for both experiments). Because there is no significant improvement in the performance of the model using a fine GFS resolution (i.e. 0.25⁰ x 0.25⁰) it is decided to use **GFS at 0.50⁰ x 0.50⁰** for optimising the time execution of the model in the daily system.

To conclude, after the revision of the results of the sensitivity tests conducted with the Multiscale Online Nonhydrostatic AtmospheRe CHemistry model (MONARCH), it is proposed the following model configuration to replace the current operational version of the WMO Barcelona Dust Forecast Center.

- **Meteorological driver:** NMMB
- **Desert dust module:** Desert dust source function from MODIS source; Emission scheme from G01
- **Spatial domain:** North Africa, Middle East and Europe
- **Spatial resolution:** The resolution of the model is set to 0.10⁰ in the horizontal and to 40 layers extending up to approximately 15 km in the vertical.
- **Meteorological global initial and boundary conditions:** NCEP/GFS at 0.50⁰ x 0.50⁰

2.3. Benchmark's results

This new MONARCH model configuration was fully evaluated for the years 2018-2019 for dust optical depth (at 550nm, DOD) and surface concentration (i.e. PM10 and PM2.5). Here, we evaluate and discuss the results of the operational and the upgraded model simulations (i.e. **benchmark analysis**) over the operational domain, which includes Northern Africa, the Middle East and Europe (NAMEE).

2.3.1. *Model configuration*

The model configuration used is described in Section 2.1.3. For the benchmark exercise, the simulated dust distributions consist of daily runs and the initial state of the dust concentration is defined by the 24-h forecast of the previous-day model run. Only in the 'cold start' of the model, concentration is set to zero. The cold start of the model is initiated on 1st January 2017 to also include the spin-up of the soil moisture (that requires a year). The Global Forecast System (GFS) which is a global weather forecast produced by the National Centers for Environmental Prediction (NCEP) at 12UTC are used as initial meteorological conditions and boundary conditions at

intervals of 6 h. The resolution of the model is set to 0.10^0 in the horizontal and to 40 layers extending up to approximately 15 km in the vertical.

2.3.2. DOD comparison over NAMEE

The operational and upgraded MONARCH runs have been compared using dust-filtered direct-sun DOD AERONET observations (Version 3 Level 1.5) for the year 2018 (see Figure 2.3.1) and 2019 (see Figure 2.3.2). The dust-filtering is based on the Angstrom Exponent (AE, dust, DOD = AOD is considered when AE < 0.75 and non-dust situations, DOD = 0, when AE > 1.2, observations between these ranges are not included in the statistical calculations). *Please, be aware that the AERONET dust-filtering is not the same as the one included in the WMO Regional Centers websites that only considers those AERONET observations with AE < 0.60.* In addition, at those sites where the SDA AERONET products are available, the DOD upgraded MONARCH evaluation is complemented with DODcoarse, which is fundamentally associated with maritime/oceanic aerosols and desert dust. Since sea-salt is related to low AOD (< 0.03; Dubovik et al., 2002) and mainly affects coastal stations, high AOD-coarse values are mostly related to mineral dust (i.e. DODcoarse).

For DOD, both runs can reproduce the daily variability with an annual overall correlation coefficient above 0.70 (0.72 and 0.75 for 2018 and 2019 respectively for the operational run, and 0.77 and 0.76 for 2018 and 2019 respectively for the upgraded run) with higher values in long-transport regions as Southern Europe. Underestimations present in the operational run (annual MB of -0.02 for 2018 and 0 for 2019) are reduced in the upgraded version that tends to overestimate the DOD AERONET observations with annual MB of 0 for 2018 and 0.01 for 2019. As it is shown in Figure 2.3.1 and Figure 2.3.2, the upgraded run shows overestimations (MB > 0) in the Sahara and the Mediterranean for DOD.
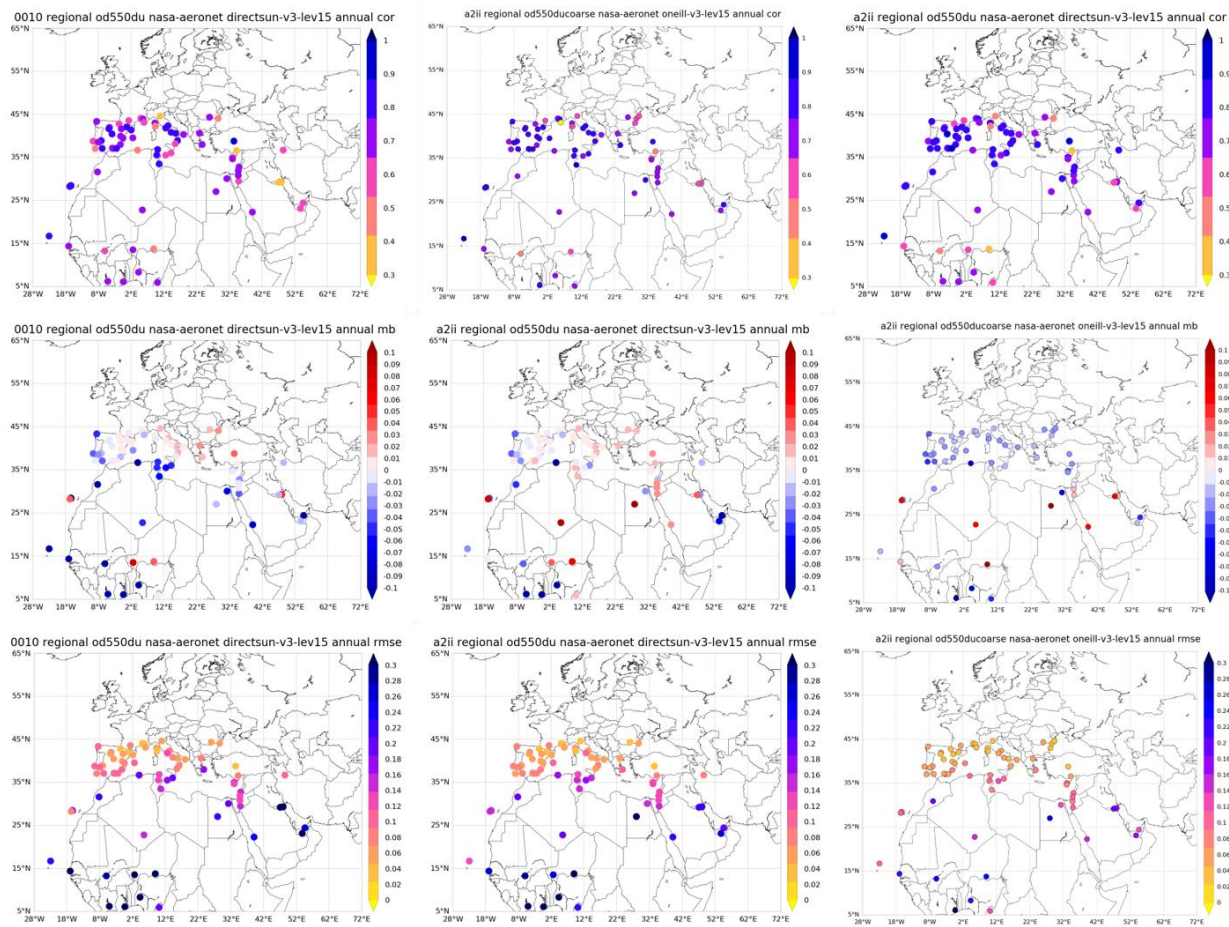
Figure 2.3.1. *Skill scores (correlation coefficient and MB) for 24-hour forecasts (at 3-hourly basis) of DOD MONARCH operational (left column), DOD MONARCH upgraded (central column) and DODcoarse MONARCH upgraded (right column) for **2018**. For DOD, dust-filtered AERONET dust observations (i.e. dust observations when AE < 0.75 and no-dust observations when AE > 1.2) is the reference meanwhile for DODcoarse, AODcoarse from SDA AERONET is considered.*

The DODcoarse comparison for the upgraded run shows an increase of the annual correlation coefficient (0.77 for 2018 and 0.74 for 2019) and a decrease in the annual MB (-0.01 for 2018 and 2019). Lower MB values (in comparison with the DOD results) are found in the Mediterranean Basin and the Middle East indicating some overestimations of the fine fractions. This will need further investigations.

Overall, the comparison with AERONET observations shows how the upgraded version of the model presents better skills scores (i.e. annual correlation coefficient increases and underestimations are reduced in the upgraded run) than the current operational configuration. Particularly, in the Middle East where the current operational configuration largely overestimates the dust optical depth (DOD, at 550 nm) during spring and summer (see Figure 2.3.4).
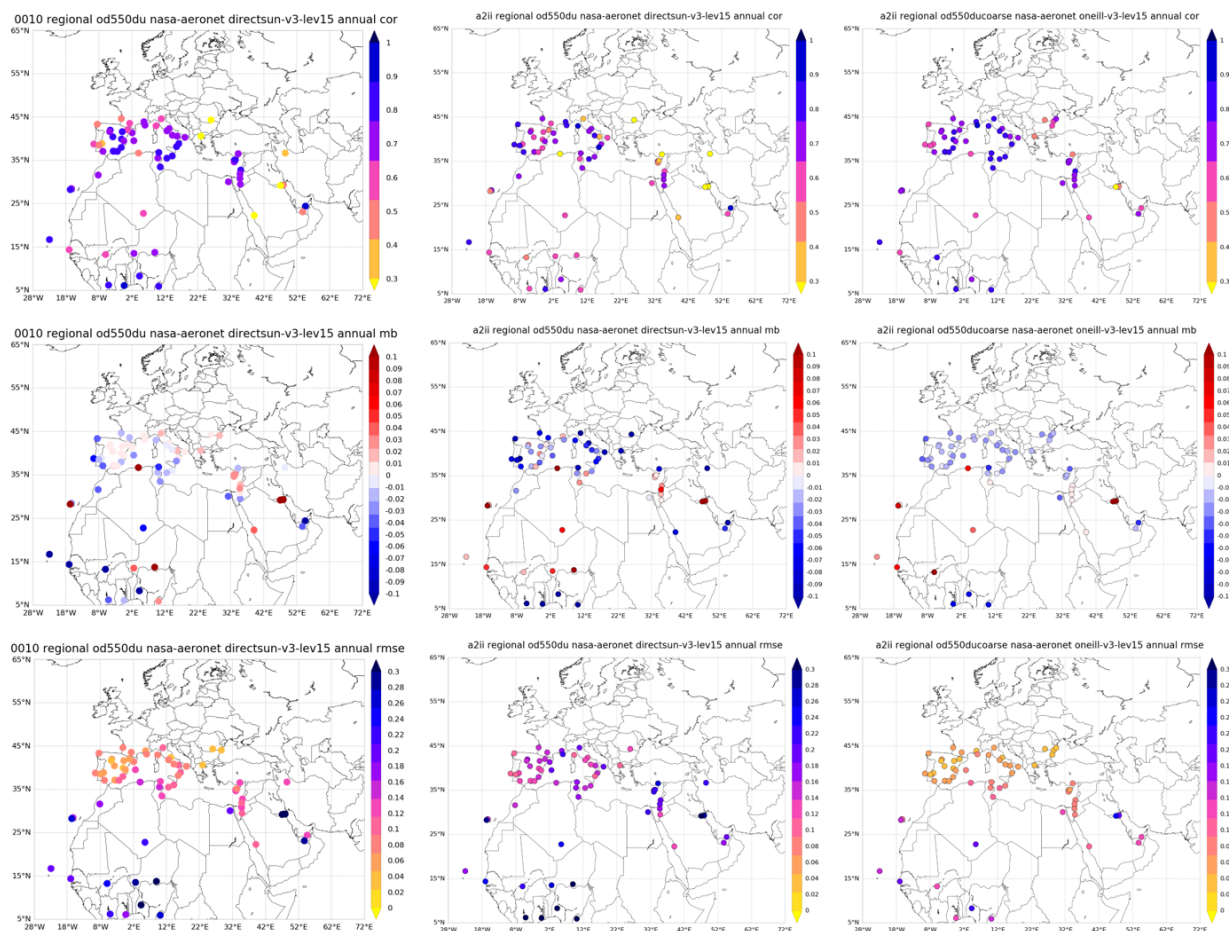
Figure 2.3.2. *Skill scores (correlation coefficient and MB) for 24-hour forecasts (at 3-hourly basis) of DOD MONARCH operational (left column), DOD MONARCH upgraded (central column) and DODcoarse MONARCH upgraded (right column) for **2019**. For DOD, dust-filtered AERONET dust observations (i.e. dust observations when AE < 0.75 and no-dust observations when AE > 1.2) is the reference meanwhile for DODcoarse, AODcoarse from SDA AERONET is considered.*
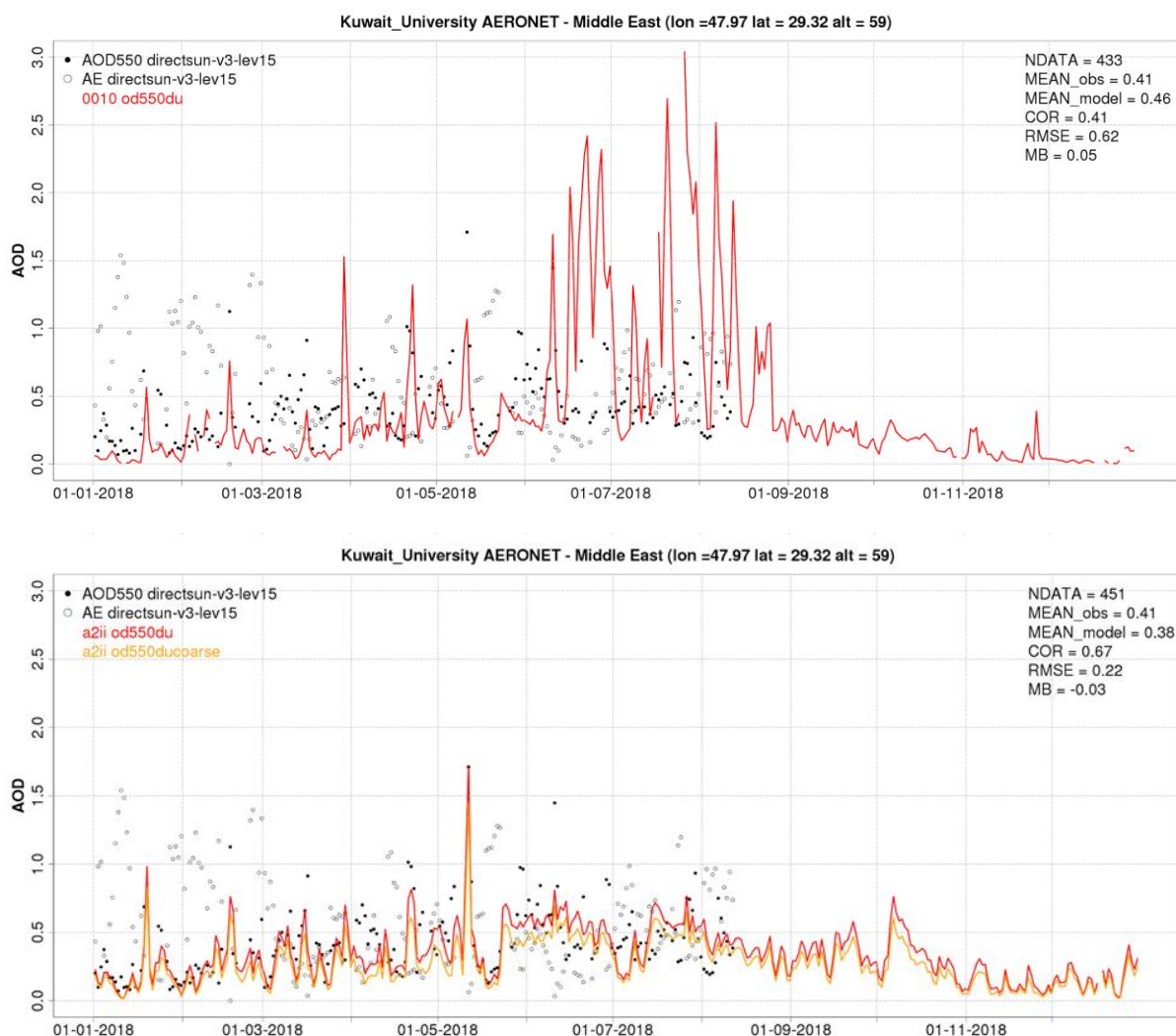
Figure 2.3.3. *AOD and Angstrom Exponent from AERONET Direct-sun (black dots), DOD MONARCH (red line) and DODcoarse MONARCH (orange line) for 2018 over Kuwait University (Middle East). Top panel: MONARCH operational. Bottom: MONARCH upgrade. Skill scores per each site and model are shown in the upper right corner (NDATA: 3-hourly pairs used for the calculations of the statistics, MEAN observations, MEAN model, COR, RMSE, MB).*

2.3.3. PM10 and PM2.5 comparison in Spain

For Spain, we include the comparison of MONARCH with the PM10 dust-filtered observations provided by the CSIC-IDAEA and available through the Spanish government website (https://www.miteco.gob.es/es/calidad-y-evaluacion-ambiental/temas/atmosfera-y-calidad-del-aire/calidad-del-aire/evaluacion-datos/fuentes-naturales/default.aspx).

Both MONARCH runs can reproduce the observed daily PM10-dust variability with annual correlation coefficients between 0.4 and 0.5 considering all the available sites. Meanwhile, the upgraded MONARCH reduces the overestimations observed in 2018 in Eastern IP, in 2019 tends

to overestimate PM10 during 2019 (see Figure 2.3.4). Overestimations in 2019 are associated with particular events (see Tefía-Puerto del Rosario in Figure 2.3.5 in which the model tends to overestimate the maximum PM10 peak despite the upgraded MONARCH version can smooth some extreme PM10 peaks that appear in the operational MONARCH version (see mid-April 2019 in Tefía-Puerto del Rosario, Lanzarote in Figure 2.7 and end-April 2018 in El Atazar, Madrid in Figure 2.3.6). These differences in the performance of the model are mainly related to the origin of the event and the associated weather conditions (e.g. if there were the presence of precipitation during the dust transport). This is currently under research. For PM2.5, the upgraded MONARCH version (see Figure 2.3.4) shows lower MB (4 µg/m3).
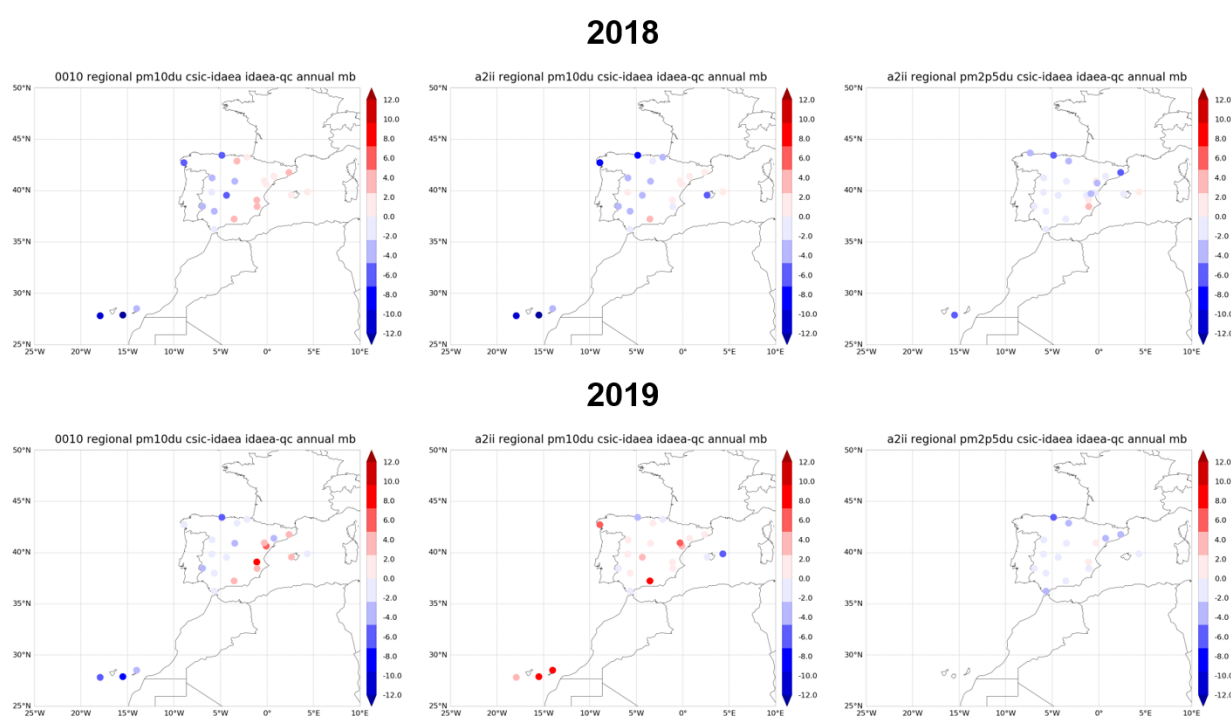
Figure 2.3.4. *Skill scores (correlation coefficient, MB and RMSE) for 24-hour forecasts of daily PM10 MONARCH operational (left column), PM10 MONARCH upgraded (central column) and PM2.5 MONARCH upgraded (right column) for 2018 and 2019. PM10-dust from CSIC-IDAEA is the reference. Daily averages from the model are calculated using 3-hourly dataset.*
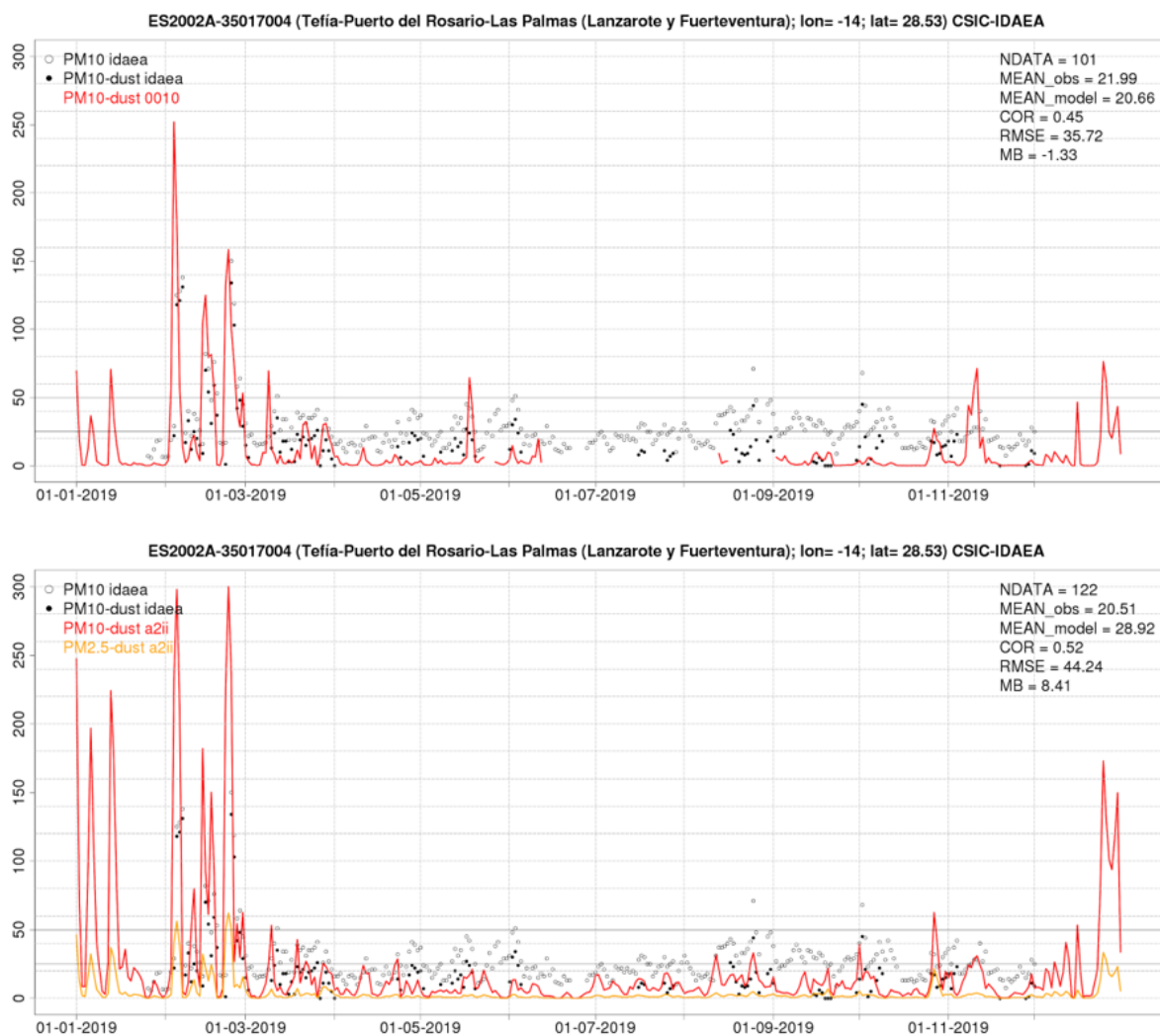
Figure 2.3.5. *Daily PM10 time series. PM10 from CSIC-IDAEA (black circles, all aerosols), PM10-dust from CSIC-IDAEA (black dots), PM10-dust MONARCH (red line) and PM2.5-dust MONARCH (orange line) for* **2019** *over* **Tefía-Puerto del Rosario** *(Lanzarote, Canary Islands, Spain). Top panel: MONARCH operational. Bottom: MONARCH upgrade. Skill scores per each site and model are shown in the upper right corner (NDATA: available days, MEAN observations, MEAN model, COR, RMSE, MB). Daily averages from the model are calculated using 3-hourly dataset.*
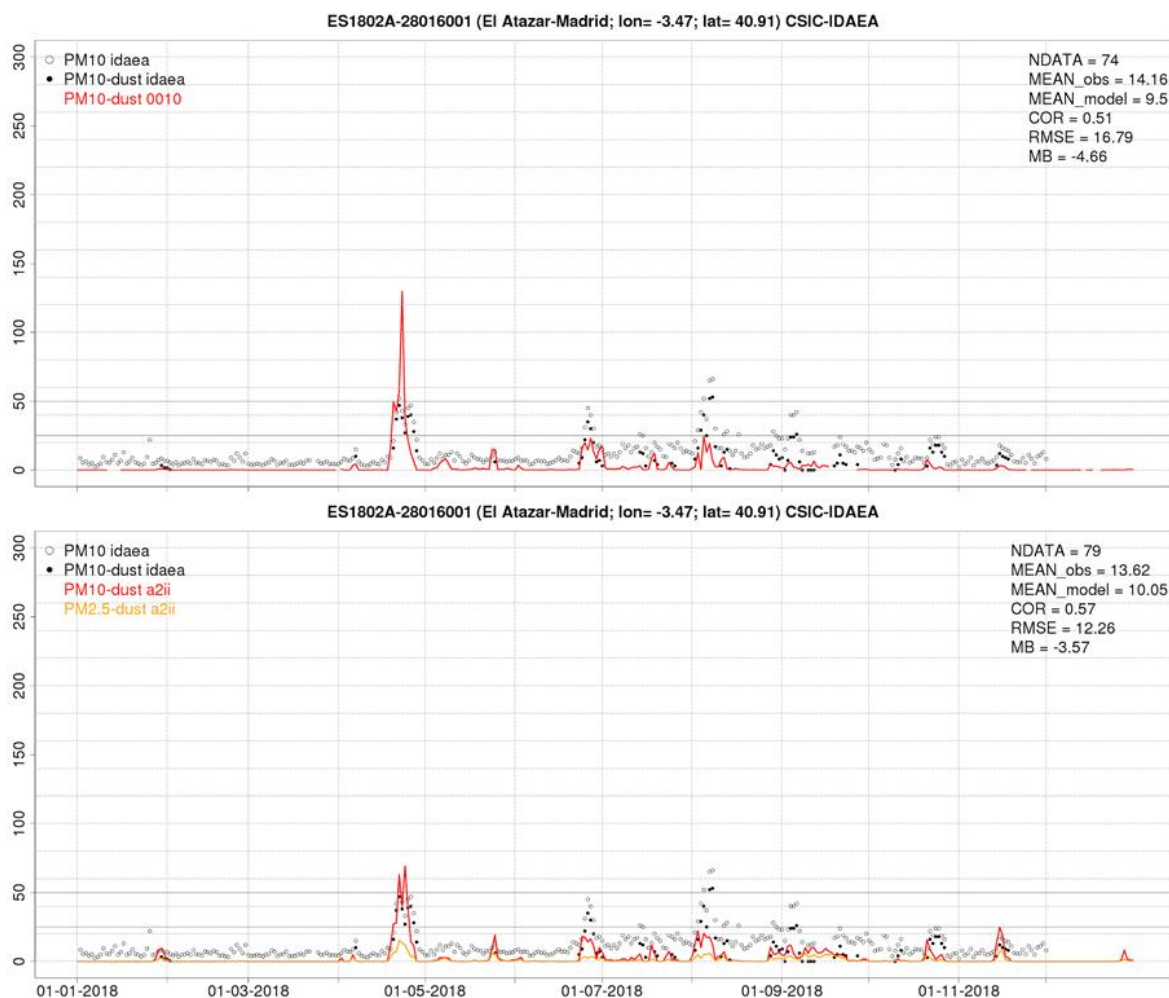
Figure 2.3.6. *Daily PM10 time series. PM10 from CSIC-IDAEA (black circles, i.e. all aerosols), PM10-dust from CSIC-IDAEA (black dots), PM10-dust MONARCH (red line) and PM2.5-dust MONARCH (orange line) for* **2018** *over* **El Atazar (Madrid, Spain)**. *Top panel: MONARCH operational. Bottom: MONARCH upgrade. Skill scores per each site and model are shown in the upper right corner (NDATA: available days, MEAN observations, MEAN model, COR, RMSE, MB). Daily averages from the model are calculated using 3-hourly dataset.*

Overall, the comparison with CSIC-IDAEA observations shows how the upgraded version of the model presents better skills scores (i.e. annual correlation coefficient increases and underestimations are reduced in the upgraded run) than the current operational configuration. Winter overestimations in the transport to the Canary Islands are under investigation.

2.4. Pre-operational results

This upgraded model version has been installed in parallel to the daily operational execution in MareNostrum4 and Nimbus (see Section 1.2). The whole workflow is running in parallel to the operational version (i.e. pre-operational phase) for finalising the implementation of the last post-processes, and for checking the stability of the runs in both machines and the results of the

model's upgrade in an operational environment. In the present section, we will revise the results of the model's upgrade in an operational environment (i.e. pre-operational phase). The period of the analysis is from **1 July to 25 November 2020,** and the model outputs are compared using AERONET as a reference. The results are summarised in Figure 2.4.1 and Figure 2.4.2.
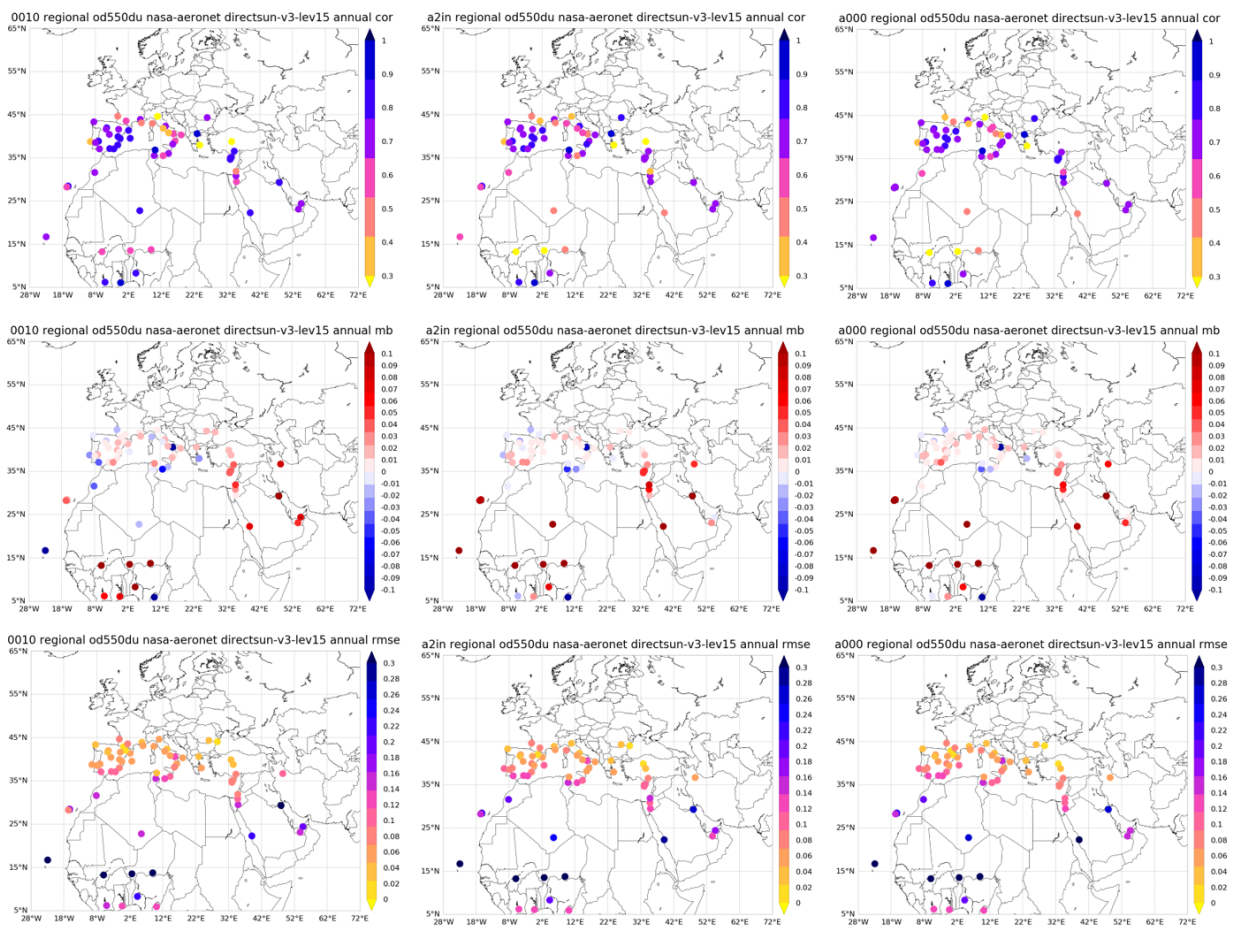
Figure 2.4.1. *Skill scores (correlation coefficient, MB and RMSE) for 24-hour forecasts (at 3-hourly basis) of DOD MONARCH operational (left column), DOD MONARCH upgraded's run in MareNostrum 4 (central column) and DOD MONARCH upgraded's run in Nimbus (right column) from 1 July to 25 November 2020. For DOD, dust-filtered AERONET dust observations (i.e. dust observations when AE < 0.75 and no-dust observations when AE > 1.2) is the reference.*
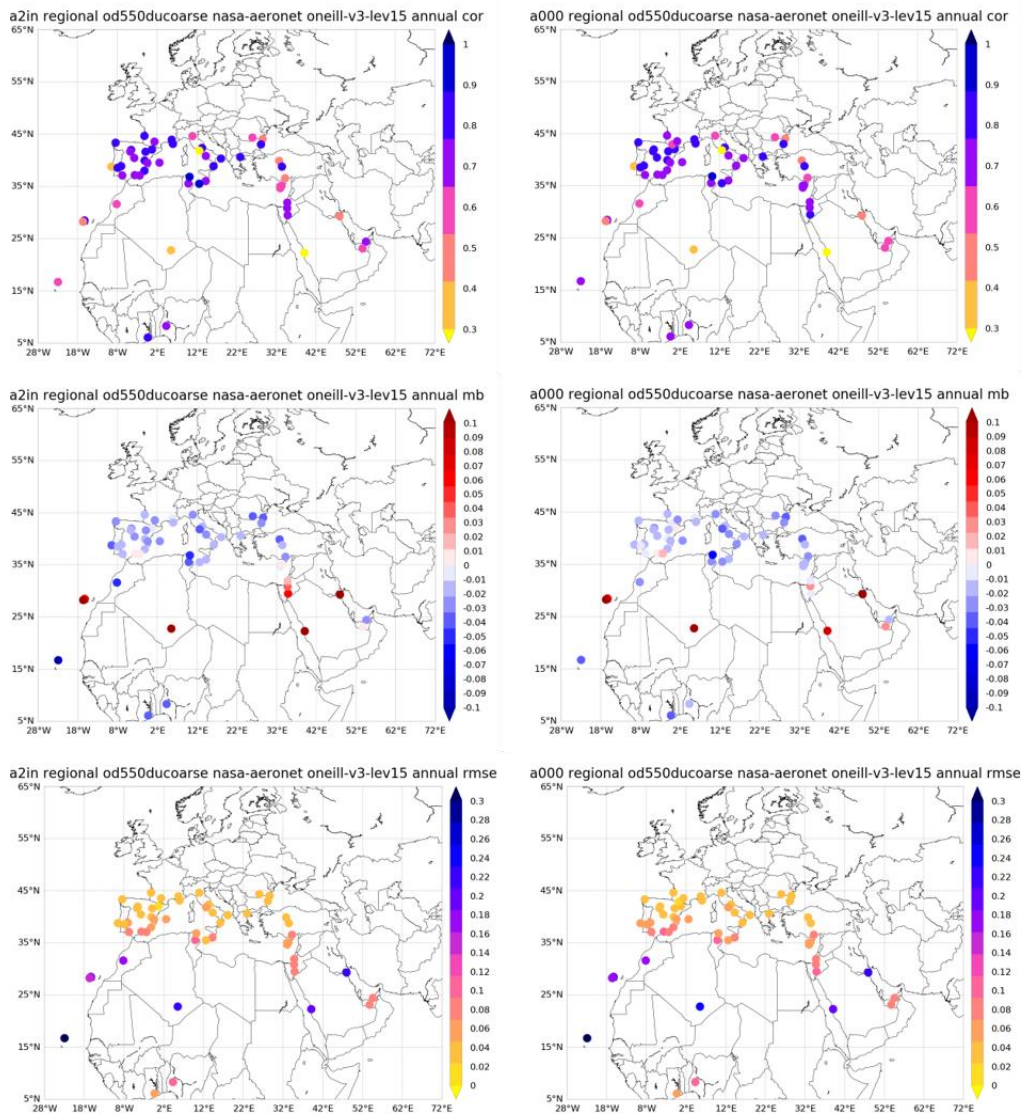
Figure 2.4.2. *Skill scores (correlation coefficient, MB and RMSE) for 24-hour forecasts (at 3-hourly basis) of DODcoarse MONARCH upgraded from **1 July to 25 November 2020**. In the left panel, they are the results of the MareNostrum 4 run, and in the right panel, the results of the Nimbus run. For DODcoarse, AODcoarse from SDA AERONET is considered.*

Overall, the results of the model in MareNostrum 4 and Nimbus are consistent with those obtained in the benchmark phase (see Section 2.2). Overestimations in the Middle East observed in the operational run are reduced in the candidate runs (see Figure 2.4.3). Also in Sahara (see Tamanarasset INM in Figure 4.2.4), both candidate runs tend to overestimate the AERONET observations as it was also observed in the benchmark phase. These Sahara overestimations are spread to the Canary Islands (see Santa Cruz de Tenerife in Figure 2.4.5). These overestimations are being the focus of further research. Otherwise, some slight differences are observed between both candidate runs. Differences are related to the available runs. As shown

in the time series of three AERONET sites (see Figure 2.4.3, Figure 2.4.4 and Figure 2.4.5), there are some gaps in both candidate runs indicating instabilities in the operation workflow manager. Moreover, it was detected a bug with the dust initial condition's implementation. If there is a failure in the execution of the model, the next run was taking the latest dust initial condition independently of the date of the run (see 1st October in Figure 2.4.4 in the MareNostum 4 run, central plot). This bug was corrected in the workflow.

Since 3 November 2020, *Autosubmit 3.12.0* was installed in MareNostrum 4 and Nimbus for overcoming the instabilities observed in the execution of both parallel runs from June to September 2020. After the *Autosubmit*'s upgrade, there are no interruptions in the execution of the model in both machines, i.e. MareNostrum 4 and Nimbus, except for MareNostrum 4 on 24th November 2020. During this day, there was technical maintenance in the BSC infrastructure.

After these technical checks, it was decided to move to operations the candidate version in December 2020.
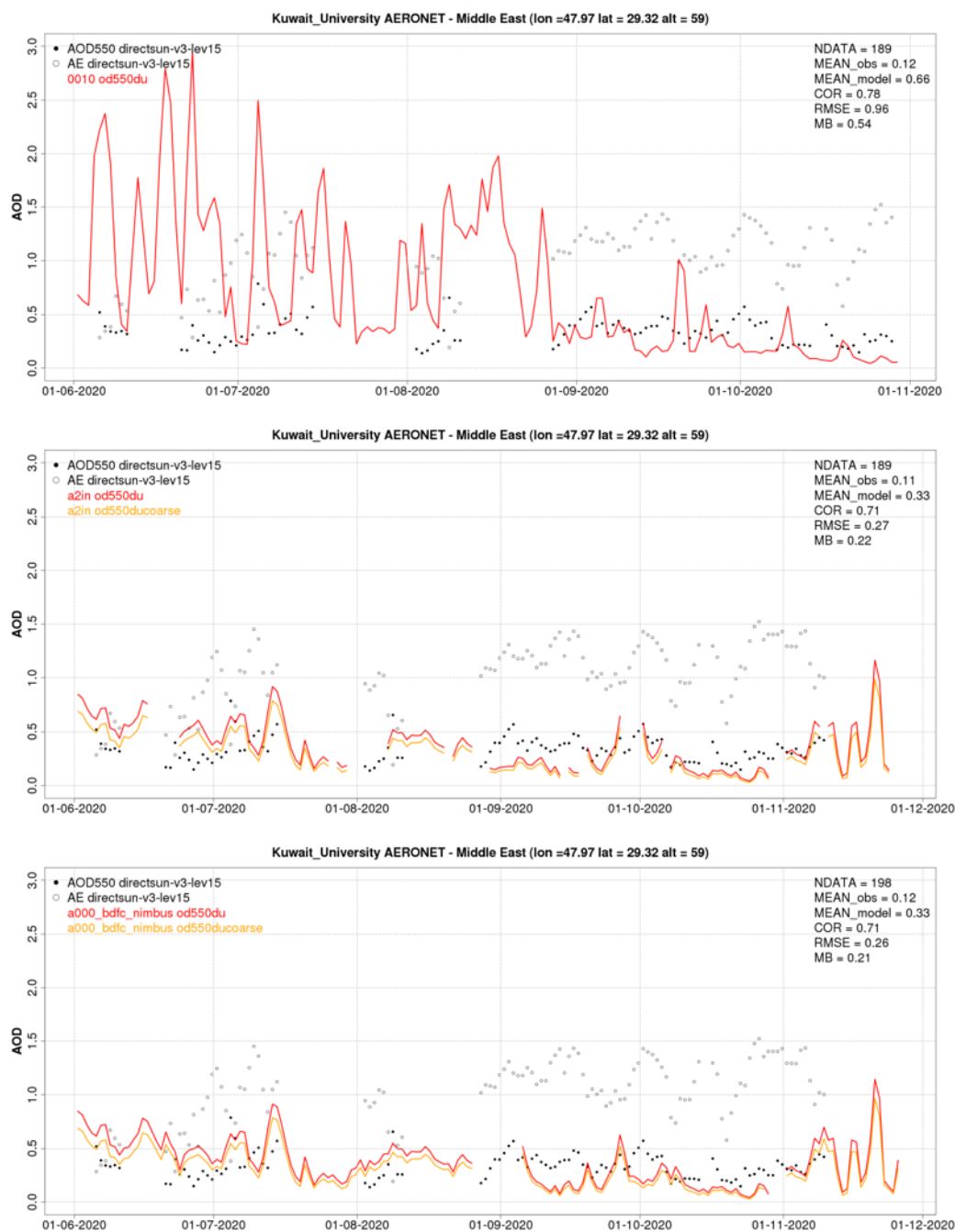
Figure 2.4.3. *AOD and Angstrom Exponent from AERONET Direct-sun (black dots), DOD MONARCH (red line) and DODcoarse MONARCH (orange line) from* **1 July to 25 November 2020** *over* **Kuwait University (Kuwait, Middle East)***. Top panel: MONARCH operational. Bottom: MONARCH upgrade. Skill scores per each site and model are shown in the upper right corner (NDATA: 3-hourly pairs used for the calculations of the statistics, MEAN observations, MEAN model, COR, RMSE, MB).*
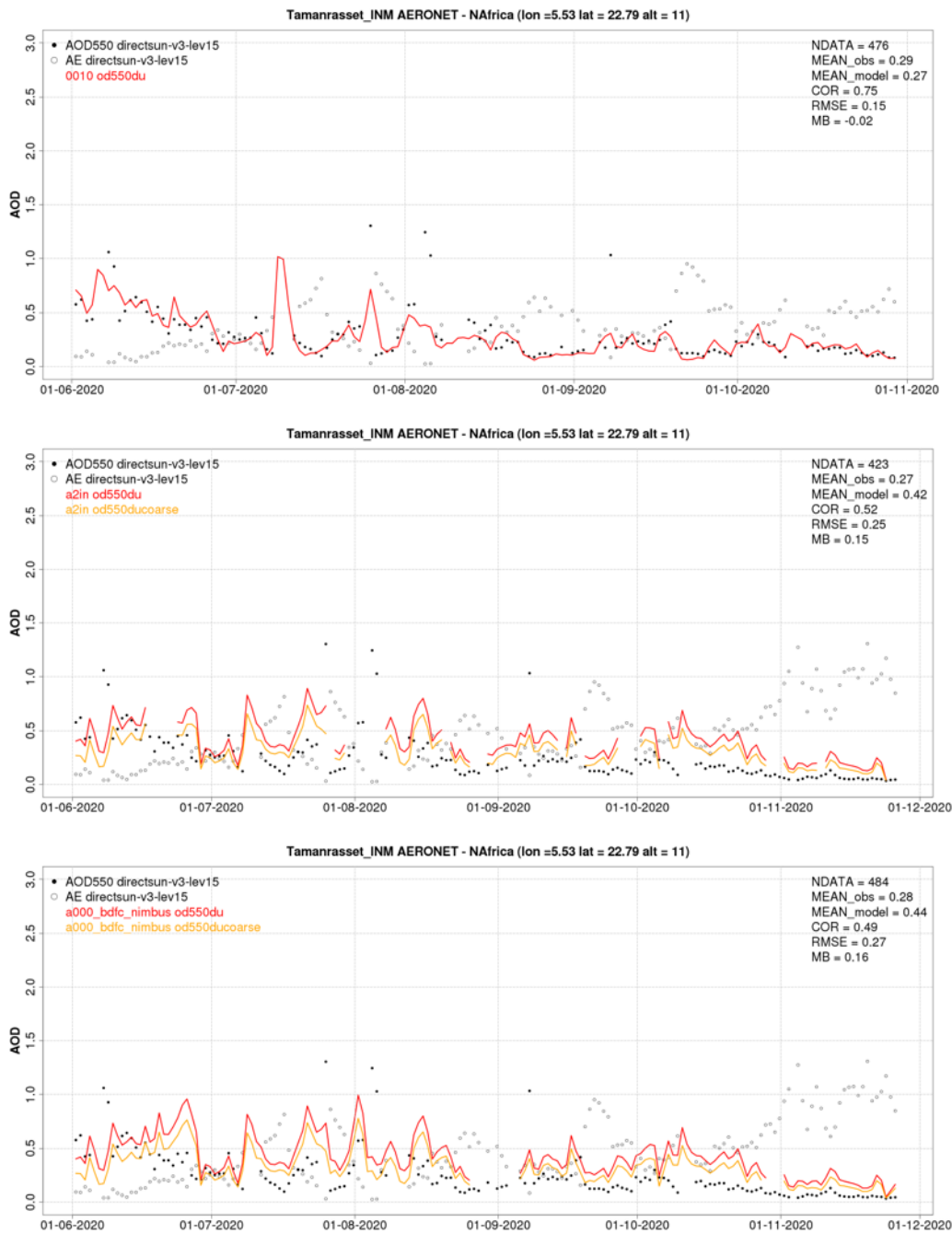
Figure 2.4.4. *AOD and Angstrom Exponent from AERONET Direct-sun (black dots), DOD MONARCH (red line) and DODcoarse MONARCH (orange line) from* **1 July to 25 November 2020** *over* **Tamanrasset INM (Algeria, Sahara)**. *Top panel: MONARCH operational. Bottom: MONARCH upgrade. Skill scores per each site and model are shown in the upper right corner (NDATA: 3-hourly pairs used for the calculations of the statistics, MEAN observations, MEAN model, COR, RMSE, MB).*
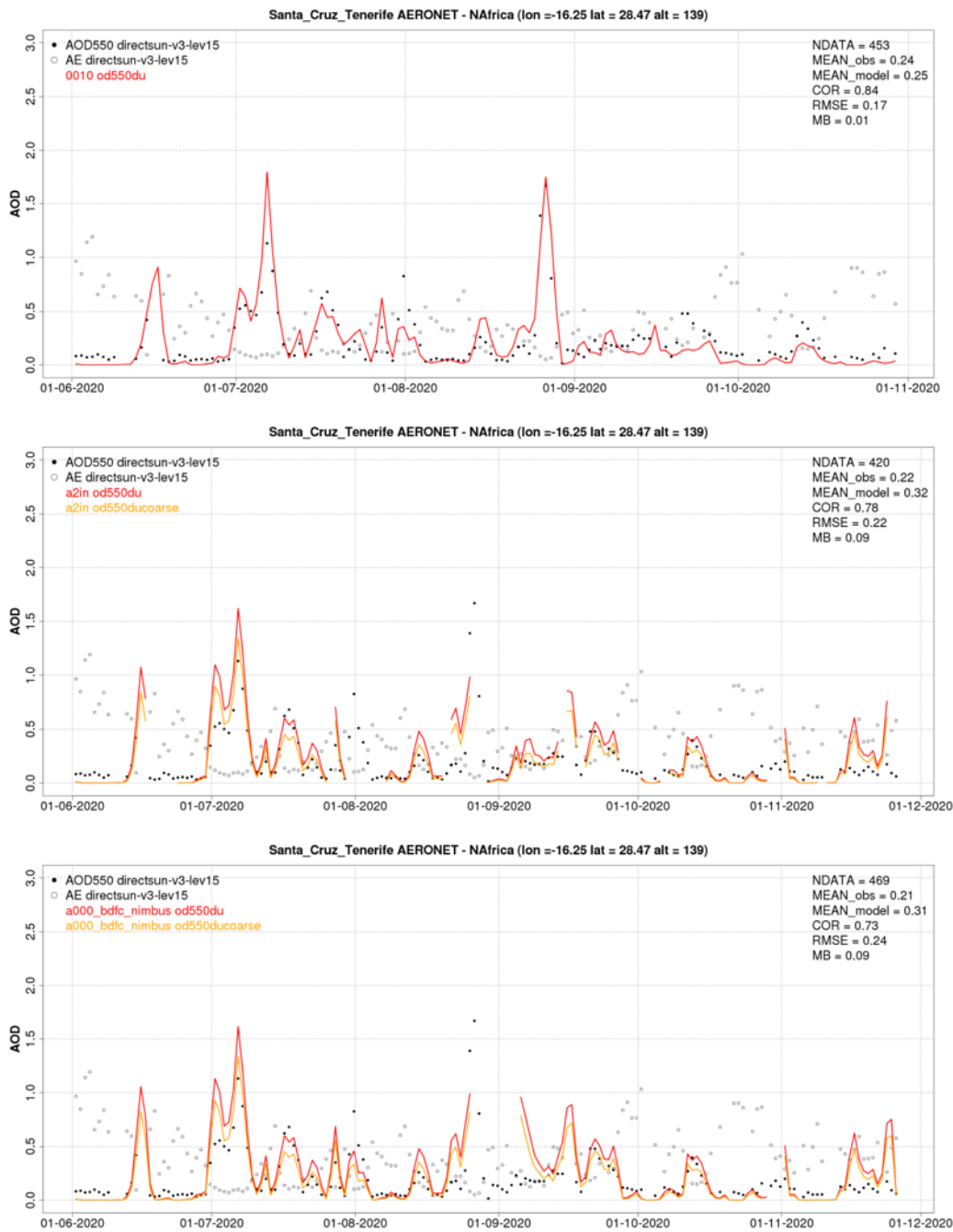
Figure 2.4.5. *AOD and Angstrom Exponent from AERONET Direct-sun (black dots), DOD MONARCH (red line) and DODcoarse MONARCH (orange line) from* **1 July to 25 November 2020** *over* **Santa Cruz de Tenerife (Canary Islands, Spain)**. *Top panel: MONARCH operational. Bottom: MONARCH upgrade. Skill scores per each site and model are shown in the upper right corner (NDATA: 3-hourly pairs used for the calculations of the statistics, MEAN observations, MEAN model, COR, RMSE, MB).*

3. References

Ackerman, S.A., Strabala, K.I., Menzel, W.P., Frey, R.A., Moeller, C.C., and Gumley, L.E., 1998. Discriminating clear sky from clouds with MODIS, J. Geophys. Res., 103, 32139–32140.

Anderson, T.L., Wu, Y., Chu, D.A., Schmid, B., Redemann, J., and Dubovik, O., 2005. Testing the MODIS satellite retrieval of aerosol fine-mode fraction. J. Geophys. Res., 110, D18204, doi:10.1029/2005JD005978.

Badia, A., & Jorba, O. (2015). Gas-phase evaluation of the online NMMB/BSC-CTM model over Europe for 2010 in the framework of the AQMEII-Phase2 project. Atmospheric Environment, 115, 657-669.

Badia, A., & Jorba, O., 2016. Gas-phase evaluation of the online NMMB/BSC-CTM model over Europe for 2010 in the framework of the AQMEII-Phase2 project. Atmospheric Environment, 115, 657-669.Badia et al. 2017;

Basart, S., Pérez García-Pando, C., Cuevas, E., Baldasano Recio, J. M., & Gobbi, P. (2009). Aerosol characterization in Northern Africa, Northeastern Atlantic, Mediterranean Basin and Middle east from direct-sun AERONET observations. Atmospheric Chemistry and Physics, 9(21), 8265-8282.

Di Tomaso, E., Schutgens, N. A. J., Jorba, O. & Pérez García-Pando, C. (2016). Assimilation of MODIS Dark Target and Deep Blue observations in the dust aerosol component of NMMB/BSC-CTM version 1.0, Geosci. Model Dev. Discuss., doi:10.5194/gmd-2016-206

Di Tomaso, E., Schutgens, N. A. J., Jorba, O., and Pérez García-Pando, C., 2017. Assimilation of MODIS Dark Target and Deep Blue observations in the dust aerosol component of NMMB/BSC-CTM version 1.0. Geosci. Model Dev., 10, 1107-1129, doi:10.5194/gmd-10-1107-2017.

Dubovik, O., Holben, B., Eck, T. F., Smirnov, A., Kaufman, Y. J., King, M. D., ... & Slutsker, I. (2002). Variability of absorption and optical properties of key aerosol types observed in worldwide locations. Journal of the atmospheric sciences, 59(3), 590-608.

Eck, T. F., Holben, B. N., Reid, J. S., Dubovik, O., Smirnov, A., O'Neill, N. T., Slutsker, I., and Kinne, S.: Wavelength dependence of optical depth of biomass burning, urban and desert dust aerosols, J. Geophys. Res., 104(D24), 31333–31350, 1999.

Eck, T. F., Holben, B. N., Dubovik, O., Smirnov, A., Goloub, P., Chen, H. B., Chatenet, B., Gomes, L., Zhang, X. Y., and Tsay, S. C.: Columnar aerosol optical properties at AERONET sites in central eastern Asia and aerosol transport to the tropical mid-Pacific, J. Geophys. Res, 110, D06202, doi:10.1029/2004JD005274, 2005.

Eck, T. F., Holben, B. N., Reid, J. S., Sinyuk, A., Dubovik, O., Smirnov, A., Giles, D., O'Neill, N. T., Tsay, S. C., and Ji, Q.: Spatial and temporal variability of column-integrated aerosol optical properties in the southern Arabian Gulf and United Arab Emirates in summer

Gao, B.-C., Kaufman, Y.J., Tanré, D., and Li, R.-R., 2002. Distinguishing tropospheric aerosols from thin cirrus clouds for improved aerosol retrievals using the ratio of 1.38μm and 1.24μm channels, Geophys. Res. Lett., 29, 1890, doi:10.1029/2002GL015475.

Ginoux, P., Chin, M., Tegen, I., Prospero, J. M., Holben, B., Dubovik, O., & Lin, S. J. (2001). Sources and distributions of dust aerosols simulated with the GOCART model. Journal of Geophysical Research: Atmospheres, 106(D17), 20255-20273.

Ginoux, P., Garbuzov, D., and Hsu, N.C., 2010. Identification of anthropogenic and natural dust sources using Moderate Resolution Imaging Spectroradiometer (MODIS) Deep Blue level 2 data, J. Geophys. Res. Atmos., 115, doi:10.1029/2009jd012398.

Ginoux, P., Prospero, J.M., Gill, T.E., Hsu, N.C., and Zhao, M., 2012. Global-Scale Attribution of Anthropogenic and Natural Dust Sources and Their Emission Rates Based on Modis Deep Blue

Aerosol Products, Rev. Geophys., 50, doi:10.1029/2012rg000388.

Gobbi, G. P., Kaufman, Y. J., Koren, I., and Eck, T. F.: Classification of aerosol properties derived from AERONET direct sun data, Atmos. Chem. Phys., 7(2), 453–458, 2007.Kim et al., 2007; Kaskaoutis et al., 2007

Guerschman, J., Scarth, P., Mcvicar, T., Renzullo, L., Malthus, T., Stewart, J.B., Rickards, J.E., and Trevithick, R., (2015). Assessing the effects of site heterogeneity and soil properties when unmixing photosynthetic vegetation, non-photosynthetic vegetation and bare soil fractions from Landsat and MODIS data. Remote Sensing of Environment. 161. 10.1016/j.rse.2015.01.021.

Haustein, K., Pérez, C., Baldasano, J. M., Jorba, O., Basart, S., Miller, R. L., ... & Washington, R. (2012). Atmospheric dust modeling from meso to global scales with the online NMMB/BSC-Dust model Part 2: Experimental campaigns in Northern Africa. Atmospheric Chemistry and Physics, 12(L03812), 2933-2958.Jorba et al. 2012;

Holben, B. N., Eck, T. F., Slutsker, I., Tanre, D., Buis, J. P., Setzer, A., ... & Lavenu, F. (1998). AERONET—A federated instrument network and data archive for aerosol characterization. Remote sensing of environment, 66(1), 1-16.

Hsu, N. C., S. C. Tsay, M. D. King, and J. R. Herman, 2006, Deep blue retrievals of Asian aerosol properties during ACE-Asia, IEEE Trans. Geosci. Remote Sens., 44, 3180–3195.

Hsu, N.C., Tsay, S.C., King, M.D., and Herman, J.R., 2004. Aerosol properties over bright-reflecting source regions. IEEE Trans. Geosci. Rem. Sens., 42(3), 557–569.

Janjic, Z., & Gall, L. (2012). Scientific documentation of the NCEP nonhydrostatic multiscale model on the B grid (NMMB). Part 1 Dynamics.

Klose, M., Y. Shao, X. Li, H. Zhang, M. Ishizuka, M. Mikami, and J. F. Leys (2014), Further development of a parameterization for convective turbulent dust emission and evaluation based on field observations, *J. Geophys. Res. Atmos.*, 119, 10,441–10,457, doi:10.1002/2014JD021688.

Kok, J. F., Mahowald, N. M., Fratini, G., Gillies, J. A., Ishizuka, M., Leys, J. F., Mikami, M., Park, M.-S., Park, S.-U., Van Pelt, R. S., and Zobeck, T. M. (2014) An improved dust emission model – Part 1: Model description and comparison against measurements, Atmos. Chem. Phys., 14, 13023-13041, https://doi.org/10.5194/acp-14-13023-2014.

Li, R.-R., Kaufman, Y.J., Gao, B.-C., and Davis, C.O., 2003. Remote sensing of suspended sediments and shallow coastal waters, IEEE Trans. Geosci. Remote Sens., 41, 559–566.

Liu, M., Westphal, D. L., Holt, T. R., and Xu, Q.: Numerical Simulation of a Low-Level Jet over Complex Terrain in Southern Iran, Mon. Weather Rev., 128(5), 1309–1327, 2000.

Marticorena, B. and Bergametti, G. (1995) Modeling the Atmospheric Dust Cycle .1. Design of a Soil-Derived Dust Emission Scheme, doi:10.1029/95jd00690.

Martins, J.V., Tanré, D., Remer, L.A., Kaufman, Y.J., Mattoo, S., and R. Levy, 2002. MODIS cloud screening for remote sensing of aerosol over oceans using spatial variability, Geophys. Res. Lett., 29, 8009, doi:10.1029/2001GL013252.

O'Neill, N. T., Eck, T. F., Smirnov, A., Holben, B. N., & Thulasiraman, S. (2003). Spectral discrimination of coarse and fine mode optical depth. Journal of Geophysical Research: Atmospheres, 108(D17).

Pérez, C., Haustein, K., Janjic, Z., Jorba, O., Huneeus, N., Baldasano, J. M., ... & Perlwitz, J. P. (2011). Atmospheric dust modeling from meso to global scales with the online NMMB/BSC-Dust model–Part 1: Model description, annual simulations and evaluation. Atmospheric Chemistry and Physics, 11(24), 13001-13027.

Pérez, C., Nickovic, S., Pejanovic, G., Baldasano, J. M., & Özsoy, E. (2006). Interactive dust-radiation modeling: A step to improve weather forecasts. Journal of Geophysical Research: Atmospheres, 111(D16).

Prigent, C., C. Jimenez, and J. Catherinot (2012), Comparison of satellite microwave backscattering (ascat) and visible/near-infrared reflectances (parasol) for the estimation of aeolian aerodynamic roughness length in arid and semi-arid regions, Atmospheric Measurement Techniques Discussions, 5, 2933-

2957, doi:10.5194/amtd-5-2933-2012.

Pu, B., and Ginoux, P., 2016. The impact of the Pacific Decadal Oscillation on springtime dust activity in Syria, Atmos. Chem. Phys., 16, 13431–13448, doi:10.5194/acp-16-13431-2016.

Remer, L.A., Kaufman, Y.J., Tanre, D., Mattoo, S., Chu, D.A., Martins, J.V., Li, R.R., Ichoku, C., Levy, R.C., Kleidman, R.G., Eck, T.F., Vermote, E., Holben, B.N., 2005. The MODIS aerosol algorithm, products, and validation, J. Atmos. Sci., 62(4), 947–973.

Schuster, G. L., Dubovik, O., and Holben, B. N.: Angstrom exponent and bimodal aerosol size distributions, J. Geophys. Res, 111, D07207, doi:10.1029/2005JD006328, 2006.

Shao, Y. (2001), A model for mineral dust emission, *J. Geophys. Res.*, 106(D17), 20239–20254, doi:10.1029/2001JD900171.

Shao, Y. (2004), Simplification of a dust emission scheme and comparison with data, *J. Geophys. Res.*, 109, D10202, doi:10.1029/2003JD004372.

Shao, Y., M. Ishizuka, M. Mikami, and J. F. Leys (2011), Parameterization of size-resolved dust emission and validation with measurements, *J. Geophys. Res.*, 116, D08203, doi:10.1029/2010JD014527.

Smirnov, A., Holben, B. N., Eck, T. F., Dubovik, O., & Slutsker, I. (2000). Cloud-screening and quality control algorithms for the AERONET database. Remote sensing of environment, 73(3), 337-349.

Spada, M. (2015). Development and evaluation of an atmospheric aerosol module implemented within the NMMB/BSC-CTM.

Spada, M., Jorba, O., Pérez García-Pando, C., Janjic, Z., & Baldasano, J. M. (2013). Modeling and evaluation of the global sea-salt aerosol distribution: sensitivity to size-resolved and sea-surface temperature dependent emission schemes. Atmospheric Chemistry and Physics, 13(23), 11735-11755.